

# Differentiating $U(1)'$ supersymmetric models with right sneutrino and neutralino dark matter

Jack Y. Araz,<sup>1,\*</sup> Mariana Frank,<sup>1,†</sup> and Benjamin Fuks<sup>2,3,4,‡</sup>

<sup>1</sup>*Concordia University 7141 Sherbrooke St. West, Montreal, QC, CANADA H4B 1R6*

<sup>2</sup>*Sorbonne Universités, Université Pierre et Marie Curie (Paris 06), UMR 7589, LPTHE, F-75005 Paris, France*

<sup>3</sup>*CNRS, UMR 7589, LPTHE, F-75005, Paris, France*

<sup>4</sup>*Institut Universitaire de France, 103 boulevard Saint-Michel, 75005 Paris, France*

(Dated: October 5, 2018)

We perform a detailed analysis of dark matter signals of supersymmetric models containing an extra  $U(1)'$  gauge group. We investigate scenarios in which either the right sneutrino or the lightest neutralino are phenomenologically acceptable dark matter candidates and we explore the parameter spaces of different supersymmetric realisations featuring an extra  $U(1)'$ . We impose consistency with low energy observables, with known mass limits for the superpartners and  $Z'$  bosons, as well as with Higgs boson signal strengths, and we moreover verify that predictions for the anomalous magnetic moment of the muon agree with the experimental value and require that the dark matter candidate satisfies the observed relic density and direct and indirect dark matter detection constraints. For the case where the sneutrino is the dark matter candidate, we find distinguishing characteristics among different  $U(1)'$  mixing angles. If the neutralino is the lightest supersymmetric particle, its mass is heavier than that of the light sneutrino in scenarios where the latter is a dark matter candidate, the parameter space is less restricted and differentiation between models is more difficult. We finally comment on the possible collider tests of these models.

## 1. INTRODUCTION

Supersymmetry is one of the most attractive theories of physics beyond the Standard Model (SM). It introduces a viable space-time extension, provides a natural solution to the hierarchy problem, allows for gauge coupling unification at a single Grand Unified scale, and, last but not least, it predicts a stable, neutral lightest supersymmetric particle (LSP) as a realistic weakly interacting massive particle dark matter (DM) candidate. But despite the numerous appealing aspects, low-energy supersymmetry (SUSY) is plagued by one overwhelming failure: no compelling evidence for it is seen at the LHC. This imposes stringent constraints on the masses of any supersymmetric coloured particle. Under simplified assumptions, gluino and first and second generation squark masses of less than 2 TeV are for instance excluded for a large variety of LSP masses [1–3]. The absence of any light superpartners so far hence puts the theory in serious conflict with electroweak naturalness [4, 5]. However, most searches are based on the minimal supersymmetric scenario whose parameter space left to explore at the LHC is rapidly shrinking. In addition, the minimal model suffers from serious fine-tuning problems induced by the discovery of ATLAS [6] and CMS [7] collaborations of a scalar particle with a mass of 125 GeV and with the expected properties of a Standard Model Higgs boson. On one hand, it is important to be precise enough in the measurements of the properties of the new scalar particle in order to confirm its nature as the SM Higgs boson responsible for electroweak symmetry breaking (EWSB). On the other hand, the Higgs boson mass must be compatible with the requirements imposed by supersymmetry at the expense of moving the SUSY scale above TeV energies. This relatively heavy Higgs boson mass imposes indirect pressures on the supersymmetric spectrum. For instance, there is a strong tension between LHC measurements and the need for a fine-tuning that can be as large as 300 or more to accommodate a viable EWSB mechanism in case of heavy higgsinos. It is nonetheless possible to get viable scenarios with lighter higgsinos and a less extreme fine-tuning in some corners of the parameter space [8, 9].

One could assume that supersymmetry does not manifest itself as the minimal supersymmetric standard model (MSSM), but feature instead an extended gauge symmetry. This implies the presence of additional new particles that could alter the exclusion limits derived in particular from measurements at the LHC in proton-proton collisions at centre-of-mass energies  $\sqrt{s}$  of 7, 8 and 13 TeV. Ideally, the new model would preserve all the attractive features of the MSSM, resolve some of its outstanding issues, and allow for a parameter space distinct for that of the MSSM in

\*Electronic address: [jack.araz@concordia.ca](mailto:jack.araz@concordia.ca)

†Electronic address: [mariana.frank@concordia.ca](mailto:mariana.frank@concordia.ca)

‡Electronic address: [fuks@lpthe.jussieu.fr](mailto:fuks@lpthe.jussieu.fr)

some regions. One possible source of difference between an extended SUSY model and the MSSM could be in the viable options for the LSP. In its minimal incarnation, supersymmetry has one possible dark matter candidate, the neutralino which can be an arbitrary admixture of binos, winos and higgsinos.

Dark matter searches can play an important role as probes for physics beyond the SM, especially as providers of indirect information on the spectrum of the models under investigation. We rely on these observations to investigate the opportunities for natural DM candidates offered by extended supersymmetric scenarios and to make use of dark matter data as a testing ground for extended SUSY models. In one of the simplest extensions of the MSSM, the gauge group is enlarged by an extra  $U(1)'$  symmetry. This model minimally introduces a new gauge boson, a new singlet Higgs field, and a right-handed neutrino, together with their superpartners. The right-handed sneutrino can be the LSP and a viable DM candidate in particular thanks to its interactions with the new gauge boson. This contrasts with the MSSM where left-handed scalar neutrinos, which do not partake in strong and electromagnetic interactions, cannot be possible candidates for DM as their interactions with the  $Z$  boson yield too high annihilation cross sections [10]. In addition, the lightest neutralino, that can also be an acceptable DM candidate, can exhibit novel properties due to its possible  $U(1)'$  bino component. This would lead to additional annihilation channels which may imply some dissimilarities with the MSSM neutralino LSP.

The possibility of adding an extra  $U(1)'$  gauge symmetry to the SM is well-motivated in superstring constructions [11], Grand Unified Theories (GUTs) [12], models of dynamical symmetry breaking [13], little Higgs models [14, 15], and setups with large extra dimensions [16]. Extra  $U(1)'$  groups generally arise from the breaking of an  $SO(10)$  or  $E_6$  symmetry to the SM gauge symmetry. In supersymmetry,  $U(1)'$  models also offer a solution to the MSSM fine-tuning issue that is mainly driven by the bilinear  $\mu$  term of the superpotential. This term is indeed simultaneously responsible for the Higgs boson mass and for the higgsino masses. In the MSSM, higgsinos are expected to be light, of  $\mathcal{O}(100)$  GeV, while predictions for a Higgs boson mass of about 125 GeV require supersymmetric masses of  $\mathcal{O}(1)$  TeV or more. This raises questions about the nature of the  $\mu$  parameter.  $U(1)'$  extensions of MSSM (UMSSM) suggest a solution to the so-called  $\mu$ -problem by the introduction of an effective  $\mu_{\text{eff}}$  parameter dynamically generated by the vacuum expectation value (VEV) of a new scalar field  $S$  responsible for breaking the  $U(1)'$  symmetry [17, 18]. While this resolution of the  $\mu$  problem is similar to the one provided in the next-to-minimal supersymmetric standard model (NMSSM) [19], the  $U(1)'$  symmetry additionally prevents from the appearance of cosmological domain walls [20]. Moreover, extra desirable features of UMSSM models are the absence of rapid proton decay operators (of dimension four), the protection of all fields by chirality and supersymmetry from acquiring high-scale masses, consistency with anomaly cancellation, gauge-coupling unification, as well as family universality that allow us to avoid flavour-changing neutral current constraints [21].

The aim of this article is to present a comprehensive study of all  $U(1)'$  models emerging from the breaking of an  $E_6$  symmetry in contexts where either a scalar neutrino or the lightest neutralino is the LSP. The former is not a possibility available in the MSSM, and, as we shall see, not the most natural solution in UMSSM models. There however exists a large variety of UMSSM realisations where the lightest sneutrino, which contains a dominant right-handed sneutrino component, is the LSP and where the observed dark matter abundance can be explained while satisfying other experimental constraints. This contrasts with left-handed sneutrino LSP scenarios which are excluded, as in the MSSM, by a non-zero sneutrino hypercharge that leads to a too efficient DM annihilation via a  $Z$ -boson exchange in the early Universe, and thus to a relic abundance lower than the  $\Omega_{\text{DM}} h^2$  value measured by the WMAP [22] and Planck [23] satellites. We explore the UMSSM parameter space consistent with either a sneutrino or a neutralino LSP, impose constraints from dark matter relic abundance and direct detection experiments, and then investigate potential signals of the viable scenarios at the LHC. We also address the compatibility of acceptable setups with measurements of the anomalous magnetic moment of the muon  $(g-2)_\mu$ . The differences between the two (sneutrino and neutralino LSP) scenarios are outlined and we especially emphasise the challenges originating from the fact that for most of the parameter space for which dark matter constraints are satisfied, the expected LHC signals are not visible, while benchmark setups yielding LHC signals that could be extracted from the SM background fail to satisfy dark matter constraints.

Whereas previous phenomenological studies in specific UMSSM constructions have appeared in Refs. [24–34], our analysis features new ingredients. It encompasses *all* possible  $U(1)'$  symmetries arising from the breaking of an  $E_6$  symmetry, with the goal of determining characteristic signals which discriminate them. We moreover include all constraints arising from low-energy phenomena, updated results from the  $Z'$  boson searches and from Higgs boson signal strength data. More practically, we first perform a scan of the parameter space and then derive the regions of the parameter space consistent with a viable sneutrino or neutralino dark matter candidate. We then investigate the various signals that could arise from dark matter experiments in order to pinpoint possible genuine differences between the UMSSM realisations.

Our work is organised as follows. We review the properties of the supersymmetric models featuring an extra  $U(1)$  symmetry, or UMSSM models, in Sec. 2. We then explore the corresponding parameter space and determine the regions that exhibit a compatibility with the Higgs boson signal strength and low-energy data in Sec. 3, imposing the

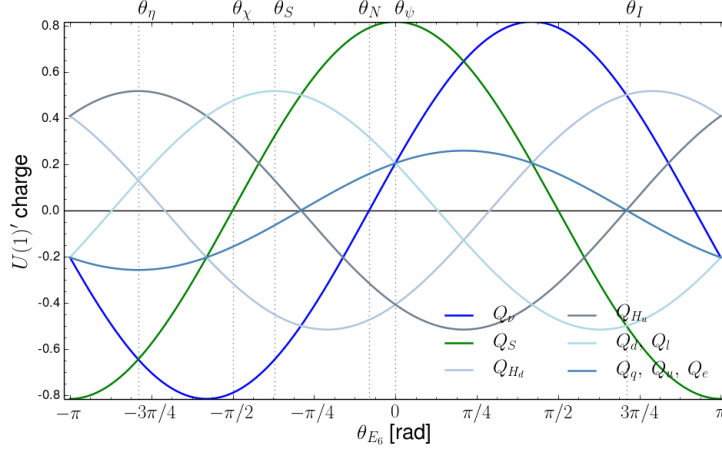


FIG. 1: Variation of the  $U(1)'$  charges of the various UMSSM superfields as a function of the  $\theta_{E_6}$  mixing angle. The standard  $U(1)'_\eta$ ,  $U(1)'_\chi$ ,  $U(1)'_S$ ,  $U(1)'_N$ ,  $U(1)'_\psi$  and  $U(1)'_I$  models are identified by dotted vertical lines.

LSP to be either a sneutrino or a neutralino. We next consider the associated  $Z'$  boson phenomenology in Sec. 3.3 and the implications for the anomalous magnetic moment of the muon in Sec. 3.4. In Sec. 4, we focus on scenarios with a right sneutrino LSP and analyse the dependence of the DM relic density on the  $Z'$  boson mass as well as direct and indirect DM detection experiment signals. In Sec. 5, we investigate cases where the neutralino is the LSP and again put an emphasis on the DM relic density, direct and indirect detection constraints. We finally discuss the prospects for observing UMSSM scenarios at colliders in Sec. 6. We summarise our findings and conclude in Sec. 7.

## 2. UMSSM MODELS

In this section, we briefly review the theoretical framework of minimal  $U(1)'$ -extended supersymmetric models that has been extensively discussed in Refs. [18, 26, 35]. The presence of the additional gauge group introduces one extra neutral gauge boson  $Z'$  of mass  $M_{Z'}$  together with the corresponding gaugino superpartner  $\lambda_{\tilde{Z}'}$ . In their simplest incarnations, UMSSM models also requires the presence of an additional electroweak singlet superfield  $S \equiv (s, \tilde{s})$ , charged under the  $U(1)'$  symmetry, that is responsible for the breaking of the extended symmetry group down to the electroweak group. The model field content moreover includes two weak doublets of quark ( $Q \equiv (q, \tilde{q})$ ) and lepton ( $L \equiv (l, \tilde{l})$ ) chiral supermultiplet as well as four weak singlets of up-type quark ( $U \equiv (u, \tilde{u})$ ), down-type quark ( $D \equiv (d, \tilde{d})$ ), charged lepton ( $E \equiv (e, \tilde{e})$ ) and right neutrino ( $N \equiv (\nu_R, \tilde{\nu}_R)$ ) chiral supermultiplets. The Higgs sector contains, in addition to the  $S$  singlet, two weak doublets of Higgs supermultiplets ( $H_u \equiv (\tilde{h}_u, h_u)$  and  $H_d \equiv (\tilde{h}_d, h_d)$ ), and the gauge sector is similar to the one of the MSSM except for the  $U(1)'$  field. It thus includes a QCD ( $G \equiv (g, \lambda_{\tilde{G}})$ ), weak ( $W \equiv (w, \lambda_{\tilde{W}})$ ) and hypercharge ( $B \equiv (b, \lambda_{\tilde{B}})$ ) gauge supermultiplets.

There are several possibilities for defining the extra  $U(1)'$  symmetry. The most commonly used parameterisation emerges from considering a linear combination of the maximal subgroups  $U(1)'_\psi$  and  $U(1)'_\chi$  resulting from the breaking of a grand unified  $E_6$  gauge group [36],

$$E_6 \longrightarrow SO(10) \otimes U(1)'_\psi \longrightarrow \left( SU(5) \otimes U(1)'_\chi \right) \otimes U(1)'_\psi . \quad (2.1)$$

Introducing a mixing angle  $\theta_{E_6}$ , a general  $U(1)'$  charge operator can be written from the respective  $U(1)'_\psi$  and  $U(1)'_\chi$  charge operators  $Q'_\psi$  and  $Q'_\chi$  as

$$Q'(\theta_{E_6}) = Q'_\psi \cos \theta_{E_6} - Q'_\chi \sin \theta_{E_6} . \quad (2.2)$$

In Fig. 1 we present the variation of the  $U(1)'$  charges of the UMSSM quark, lepton and Higgs superfields as functions of the mixing angle  $\theta_{E_6}$  that will be a key parameter of our analysis. We identify by vertical lines the anomaly-free  $U(1)'$  group choices denoted by  $U(1)'_\eta$ ,  $U(1)'_\chi$ ,  $U(1)'_S$ ,  $U(1)'_N$ ,  $U(1)'_\psi$  and  $U(1)'_I$ , and give the corresponding charge and mixing angle values in Table I.

	$2\sqrt{10}Q'_\chi$	$2\sqrt{6}Q'_\psi$	$2\sqrt{15}Q'_\eta$	$2\sqrt{15}Q'_S$	$2Q'_I$	$2\sqrt{10}Q'_N$
$\theta_{E_6}$	$-\pi/2$	0	$\arccos(\sqrt{5/8}) - \pi$	$\arctan(\sqrt{15/9}) - \pi/2$	$\arccos(\sqrt{5/8}) + \pi/2$	$\arctan \sqrt{15} - \pi/2$
$Q_{q,u,e}$	-1	1	-2	-1/2	0	1
$Q_{d,l}$	3	1	1	4	-1	2
$Q_\nu$	-5	1	-5	-5	1	0
$Q_{H_u}$	2	-2	4	1	0	2
$Q_{H_d}$	-2	-2	1	-7/2	1	-3
$Q_S$	0	4	-5	5/2	-1	5

TABLE I:  $U(1)'$  charges of the UMSSM quark ( $Q_q, Q_d, Q_u$ ), lepton ( $Q_l, Q_e, Q_\nu$ ) and Higgs ( $Q_{H_u}, Q_{H_d}, Q_S$ ) supermultiplets for the anomaly-free abelian group that could arise from the breaking of an  $E_6$  symmetry. The value of the mixing angle  $\theta_{E_6} \in [-\pi, \pi]$  is also indicated.

The UMSSM superpotential contains usual quarks and lepton Yukawa interactions and reads, in the presence of a right-handed neutrino superfield  $N$ ,

$$W = \mathbf{Y}_u U Q H_u - \mathbf{Y}_d D Q H_d - \mathbf{Y}_e E L H_d + \mathbf{Y}_\nu L H_u N + \lambda H_u H_d S, \quad (2.3)$$

where the four Yukawa couplings  $\mathbf{Y}_u, \mathbf{Y}_d, \mathbf{Y}_l$  and  $\mathbf{Y}_\nu$  are  $3 \times 3$  matrices in flavour space and  $\lambda$  represents the strength of the electroweak Higgs singlet and doublet interactions. All indices are understood but explicitly suppressed for simplicity. After the breaking of the  $U(1)'$  symmetry, the scalar component  $s$  of the singlet superfield gets a VEV  $v_S$  and the last superpotential term of Eq. (2.3) induces an effective  $\mu$ -term with  $\mu_{\text{eff}} = \lambda v_S / \sqrt{2}$ , allowing for the resolution of the  $\mu$ -problem inherent to the MSSM [37–41]. As in the MSSM, SUSY is softly broken via the introduction of gaugino mass terms,

$$-\mathcal{L}_{\text{soft}}^\lambda = \frac{1}{2} \left( M_1 \lambda_{\tilde{B}} \cdot \lambda_{\tilde{B}} + M_2 \lambda_{\tilde{W}} \cdot \lambda_{\tilde{W}} + M'_1 \lambda_{\tilde{Z}'} \cdot \lambda_{\tilde{Z}'} + M_3 \lambda_{\tilde{g}} \cdot \lambda_{\tilde{g}} + \text{h.c.} \right), \quad (2.4)$$

where the  $M_i$  variables denote the various mass parameters, scalar mass terms  $m_i$ ,

$$-\mathcal{L}_{\text{soft}}^\Phi = m_{H_d}^2 h_d^\dagger h_d + m_{H_u}^2 h_u^\dagger h_u + m_S^2 s^2 + m_{\tilde{Q}}^2 \tilde{q}^\dagger \tilde{q} + m_{\tilde{d}}^2 \tilde{d}^\dagger \tilde{d} + m_{\tilde{u}}^2 \tilde{u}^\dagger \tilde{u} + m_{\tilde{L}}^2 \tilde{l}^\dagger \tilde{l} + m_{\tilde{e}}^2 \tilde{e}^\dagger \tilde{e} + m_{\tilde{\nu}}^2 \tilde{\nu}_R^\dagger \tilde{\nu}_R, \quad (2.5)$$

and trilinear interactions featuring a structure deduced from the one of the superpotential,

$$-\mathcal{L}_{\text{soft}}^W = A_\lambda s h_u h_d - A_d \tilde{d}^\dagger \tilde{q} h_d - A_e \tilde{e}^\dagger \tilde{l} h_d + A_u \tilde{u}^\dagger \tilde{d} h_u + \text{h.c.}, \quad (2.6)$$

where the  $A_i$  parameters stand for the soft couplings.

After the breaking of the UMSSM gauge symmetry down to electromagnetism, all neutral components of the scalar Higgs fields get VEVs,  $\langle h_u^0 \rangle = v_u / \sqrt{2}$ ,  $\langle h_d^0 \rangle = v_d / \sqrt{2}$  and  $\langle s \rangle = v_S / \sqrt{2}$ . As a consequence, UMSSM models can easily lead to neutrino masses that are consistent with neutrino oscillation data through an implementation of a see-saw mechanism [42–45]. The exact details depend on the form of the extra  $U(1)'$  symmetry [46], and viable models can be constructed to contain Dirac-type [47] or Majorana neutrino masses [48]. The symmetry breaking mechanism additionally induces the mixing of fields carrying the same spin, colour and electric charge quantum numbers, and the gauge eigenbasis has to be rotated to the physical basis. Contrary to the MSSM where the tree-level SM-like Higgs-boson mass is bound by the  $Z$ -boson mass  $M_Z$  so that large stop masses and/or trilinear  $A_t$  couplings are required for pushing the loop corrections to a large enough value [49], the singlet field provides new tree-level  $F$ -term contributions that naturally stabilise the SM-like Higgs boson mass  $M_h$  to a greater value more easily in agreement with the measured experimental value of 125 GeV [50]. For any further details on the resulting particle spectrum, we refer to Refs. [17, 18, 27].

The UMSSM Lagrangian introduced above exhibit numerous parameters, in particular within its soft SUSY-breaking part. To reduce the dimensionality of the parameter space, we assume that the SUSY-breaking mechanism originates from minimal supergravity so that unification relations amongst the soft masses can be imposed at the GUT scale where an  $E_6$  gauge symmetry is realised. We however deviate from the most minimal model by maintaining the freedom to choose the details of the lepton and neutrino sector, which guarantees that a sneutrino could be the LSP. More details are given in the following section.



Parameter	Scanned range	Parameter	Scanned range
$M_0$	$[0, 3]$ TeV	$\mu$	$[-2, 2]$ TeV
$M_{1/2}$	$[0, 5]$ TeV	$A_\lambda$	$[-7, 7]$ TeV
$A_0$	$[-3, 3]$ TeV	$M_{Z'}$	$[1.98, 5.2]$ TeV
$\tan \beta$	$[0, 60]$	$m_{\tilde{\nu}}^2$	$[-6.8, 9]$ TeV <sup>2</sup>
$\theta_{E_6}$	$[-\pi, \pi]$	$m_{\tilde{e}, \tilde{l}}^2$	$[0, 1]$ TeV <sup>2</sup>

TABLE II: *Ranges over which we allow the free parameters of Eq. (3.1) to vary.*

Observable	Constraints	Ref.	Observable	Constraints	Ref.
$M_h$	$125.09 \pm 3$ GeV (theo)	[7]	$\chi^2(\mu)$	$\leq 70$	-
$ \alpha_{ZZ'} $	$O(10^{-3})$	[57]	$M_{\tilde{g}}$	$> 1.75$ TeV	[58]
$M_{\chi_2^0}$	$> 62.4$ GeV	[59]	$M_{\chi_3^0}$	$> 99.9$ GeV	[59]
$M_{\chi_4^0}$	$> 116$ GeV	[59]	$M_{\chi_i^\pm}$	$> 103.5$ GeV	[59]
$M_{\tilde{\tau}}$	$> 81$ GeV	[59]	$M_{\tilde{e}}$	$> 107$ GeV	[59]
$M_{\tilde{\mu}}$	$> 94$ GeV	[59]	$M_{\tilde{l}}$	$> 900$ GeV	[60]
$\text{BR}(B_s^0 \rightarrow \mu^+ \mu^-)$	$[1.1 \times 10^{-9}, 6.4 \times 10^{-9}]$	[61]	$\frac{\text{BR}(B \rightarrow \tau \nu_\tau)}{\text{BR}_{SM}(B \rightarrow \tau \nu_\tau)}$	$[0.15, 2.41]$	[62]
$\text{BR}(B^0 \rightarrow X_s \gamma)$	$[2.99, 3.87] \times 10^{-4}$	[63]			

TABLE III: *Experimental constraints imposed within our scanning procedure in order to determine the parameter space regions of interest.*

### 3. PARAMETER SPACE SCAN AND CONSTRAINTS

#### 3.1. Technical setup

We perform a scan of the UMSSM parameter space in order to determine regions in which either a sneutrino or a neutralino is the LSP and thus a potential dark matter candidate. We focus on the six anomaly-free UMSSM realisations introduced in the previous section. More precisely, we generate the particle spectrum by making use of SARAH version 4.6.0 [51] and SPHENO version 3.3.8 [52]. Predictions for the dark matter observables are then achieved with MICROMEGAS version 4.3.1 [53], and the properties of the Higgs sector are evaluated with HIGGSBOUNDS version 4.3.1 [54] and HIGGSIGNALS version 1.4.0 [55]. The interfacing of the various programmes and our numerical analysis have been implemented within the PYSLHA package, version 3.1.1 [56].

We make use of GUT-inspired relations to simplify the size of the parameter space. The considered set of free parameters is given by

$$M_{1/2}, \quad M_0, \quad m_{\tilde{e}}, \quad m_{\tilde{L}}, \quad m_{\tilde{\nu}}, \quad \tan \beta = \frac{v_u}{v_d}, \quad \mu_{\text{eff}}, \quad A_0, \quad A_\lambda, \quad Y_\nu, \quad M_{Z'} \quad \text{and} \quad \theta_{E_6}, \quad (3.1)$$

where we have enforced a unification relation at the GUT scale relating the  $U(1)'$ , hypercharge, weak and QCD gaugino soft masses  $M'_1 = M_1 = M_2 = M_3 = M_{1/2}$  as well as the hypercharge, weak and  $U(1)'$  gauge couplings  $g_1 = g_2 = g' \sqrt{3/5}$ . Constraining the SUSY scale to be below 5 TeV, renormalization group evolution implies, at the SUSY scale, that  $6M_1 \approx 3M_2 \approx M_3$ . We have moreover required that all squark soft masses and trilinear couplings respectively unify to common values  $M_0$  and  $A_0 Y_q$  at the GUT scale, the slepton and sneutrino masses  $m_{\tilde{e}}, m_{\tilde{L}}$  and  $m_{\tilde{\nu}}$  being kept independent whereas the leptonic trilinear coupling  $A_e$  is taken vanishing. The neutrino Yukawa matrix is finally fixed to a diagonal matrix with entries equal to  $10^{-11}$ .

Our parameter space investigation relies on the Metropolis-Hasting sampling method where the free parameters of Eq. (3.1) are allowed to vary in the ranges given in Table II, the lower bound on the mass of the  $Z'$  boson being the minimum value allowed for any choice of the  $U(1)'$  symmetry (and corresponds to the  $U(1)'_\eta$  case). This mass has been taken smaller than the one quoted in the 2016 Particle Data Group review [59] in order to allow for significant branching fractions for the  $Z'$  boson decays into a pair of supersymmetric particles [64]. We have retained scenarios for which the predictions for the observables listed in Table III agree with the experimental data. Constraints arising from

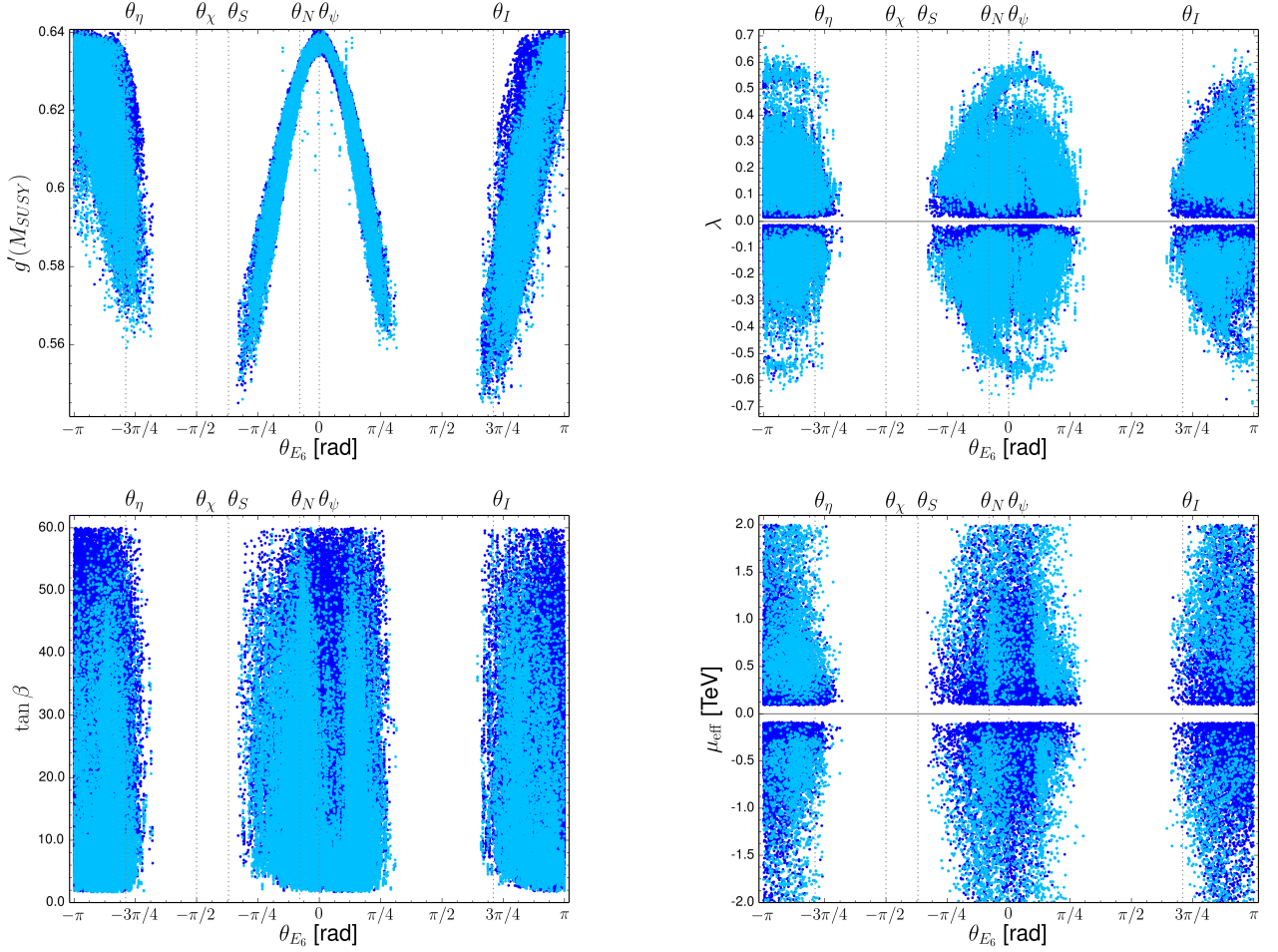


FIG. 2: Distributions in the UMSSM parameter space of the scenarios in agreement with the constraints imposed on Sec. 3.1. Results are projected into the  $(\theta_{E_6}, g')$  (upper left panel),  $(\theta_{E_6}, \lambda)$  (upper right panel),  $(\theta_{E_6}, \tan \beta)$  (lower left panel) and  $(\theta_{E_6}, \mu_{\text{eff}})$  planes. The light and dark blue points respectively represent scenarios in which the lightest sneutrino and the lightest neutralino is the LSP.

the Higgs sector, namely a theory-experiment agreement for the Higgs boson mass, the gluon and vector boson fusion Higgs boson production cross-sections, and the Higgs signal strengths, have been applied by using HIGGSBOUNDS and HIGGSSIGNALS. This is achieved by evaluating the Higgs boson production rate in the gluon and vector boson fusion channels with the SUSHI program version 1.5 [65] and by then comparing the predictions to  $\sigma(gg \rightarrow h) = 19.27^{+1.76}_{-4.44}$  pb and  $\sigma(VV \rightarrow h) = 1.55^{+0.058}_{-0.039}$  pb for a centre-of-mass energy of 8 TeV and  $\sigma(gg \rightarrow h) = 50.74^{+4.68}_{-11.6}$  pb for a centre-of-mass energy of 14 TeV [66]. We next derive a  $\chi^2(\hat{\mu})$  quantity for each, estimating the deviation from the experimental data, the sum of which we enforce to be smaller than 70. We have moreover severely restricted any possible kinetic mixing between the  $Z$  and the  $Z'$  bosons, and required that the associated mixing angle  $\alpha_{ZZ'}$  is of the order of  $10^{-3}$ . We have additionally verified that predictions for the gluino mass  $M_{\tilde{g}}$ , the neutralino and chargino masses  $M_{\tilde{\chi}_i^0}$  and  $M_{\tilde{\chi}_i^\pm}$ , the slepton masses  $M_{\tilde{e}}$ ,  $M_{\tilde{\mu}}$  and  $M_{\tilde{\tau}}$  and the stop mass  $M_t$  satisfy the experimental bounds [59]. We have also imposed constraints arising from  $B$ -physics that are related to rare  $B$ -meson decays, and checked that the three branching ratios  $\text{BR}(B_s^0 \rightarrow \mu^+ \mu^-)$ ,  $\text{BR}(B \rightarrow \tau \nu_\tau)$  and  $\text{BR}(B^0 \rightarrow X_s \gamma)$  agree with existing data.

### 3.2. General considerations and phenomenology of the Higgs sector

In Fig. 2 we present the results of our scan. We project the ensemble of accepted scenarios onto four two-dimensional planes in order to exhibit possible correlations between the  $U(1)'$  mixing angle and the  $U(1)'$  coupling  $g'$  (upper left panel), the superpotential parameter  $\lambda$  (upper right panel),  $\tan \beta$  (lower left panel) and the effective  $\mu_{\text{eff}}$  parameter

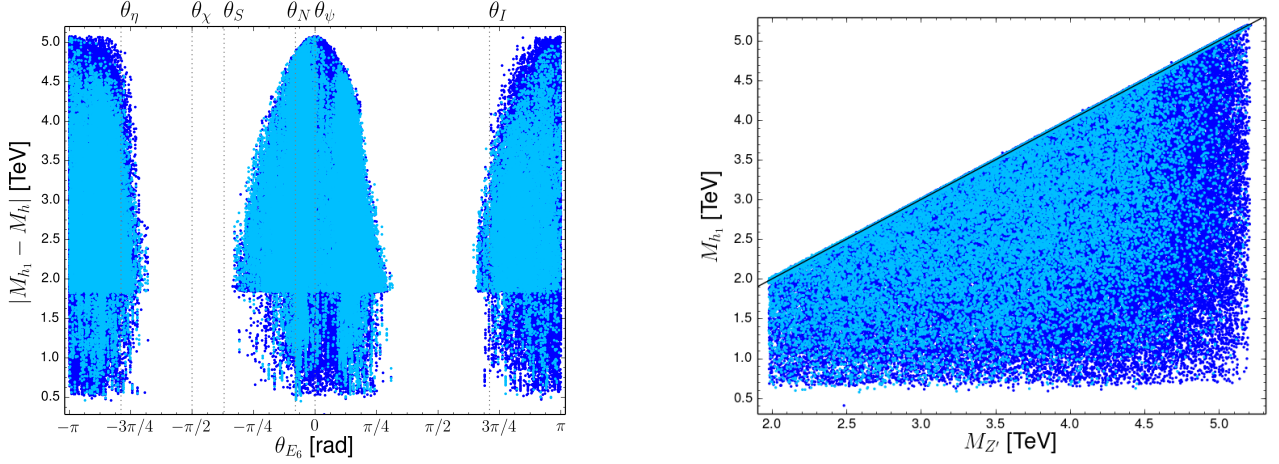


FIG. 3: Same as in Figure 2 but for projection in the  $(\theta_{E_6}, |M_{h_1} - M_h|)$  (left panel) and  $(\theta_{E_6}, M_{Z'})$  (right panel) planes.

(lower right panel). We moreover distinguish the classes of scenarios for which the LSP is a sneutrino (light blue points) and a neutralino (dark blue points).

In the upper left panel of Fig. 2, we observe that the  $g'$  coupling is in general large, which indicates that the  $U(1)'$  interactions must be strong to satisfy all the imposed constraints. Whereas the value of  $g'$  is maximal in the context of  $U(1)'_\psi$  models, it is generally highly dependent on many other parameters so that a large range of values can be probed, regardless of the precise choice of  $\theta_{E_6}$ . We however observe that  $\theta_{E_6}$  values around  $\pm\pi/2$  do not offer any option for a phenomenologically viable scenario. This in particular disfavours the  $U(1)'_S$  and  $U(1)'_\chi$  models, as already suggested by the results of Fig. 1 where the  $U(1)'$  charge of the electroweak singlet approaches zero for  $\theta_{E_6} \approx \pm\pi/2$ . In this case, the scalar field  $s$  is not sufficient to break the  $U(1)'$  symmetry and one cannot construct any predictable scenario.

The general features of the Higgs sector are then analysed in the three other panels of Fig. 2. The distribution of the  $\lambda$  parameter as a function of the  $\theta_{E_6}$  angle depicts how the weak singlet and doublets of Higgs fields mix. This information is also represented in the lower right panel of the figure where the  $\lambda$  parameter is traded for the effective  $\mu_{\text{eff}}$  parameter to which it is proportional. While all possible values (different enough from zero and below 0.6 in absolute value) are in principle possible regardless of the mixing angle value, the anomaly-free  $U(1)'_I$  model has the particularity to forbid  $|\lambda| \gtrsim 0.3$ . This stems from the structure of the  $U(1)'$  charges that are small or vanishing for several supermultiplets and the lower bound on the  $Z'$  mass in the scanning procedure that both forbid  $\lambda$  to be too large. A similar effect being also observed for  $\theta_{E_6} \approx -\pi/4$ . The  $\lambda$  parameter must additionally be sufficiently large, in absolute value, to induce a successful EWSB so that  $\lambda$  values close to zero are forbidden.

While in general a sneutrino LSP can be obtained for any value of  $\tan\beta$ , this turns out to be easier in the case of  $U(1)'_N$  models. These are scenarios where the right neutrino supermultiplet is not charged under the extended gauge symmetry, and right sneutrino masses do not therefore receive any contribution from the  $D$ -terms and mostly arise from the independent soft mass terms. As a result, one gets more freedom on  $\tan\beta$  that can be consequently lower. A similar feature, but less pronounced, can be observed for other  $\theta_{E_6}$  values where a combination of several zero  $U(1)'$  charges leads to the same conclusions.

We further investigate the properties of the Higgs sector in Fig. 3 where we present both the mass difference between the SM-like Higgs boson and the next-to-lightest Higgs boson,  $|M_{h_1} - M_h|$ , in the left panel of the figure and the dependence of  $M_{h_1}$  on the  $Z'$ -boson mass in the right panel of the figure. As the singlet VEV drives the  $Z'$  boson mass, the second lightest Higgs boson has a mass of at most roughly the  $Z'$ -boson mass and is in this case singlet-dominated. In the lighter cases, it is mostly a doublet admixture and thus MSSM-like. There are a few scenarios featuring a sneutrino LSP where the second Higgs and the  $Z'$  bosons are almost degenerate, but any hierarchy can however be realised. The second Higgs boson is however at least 500 GeV heavier than the SM-like Higgs boson, which originates from the Higgs mixing pattern and the minimum value of the singlet VEV  $v_S$  (that stems from the  $M_{Z'}$  lower limit imposed in our scan). Once again, smaller  $\lambda$  values obtained for the case of the  $U(1)'_I$  scenario impact the spectrum and  $M_{h_1}$  is in general consequently smaller, the effects driven by the large  $v_S$  value being tamed by the smaller  $\lambda$  value.

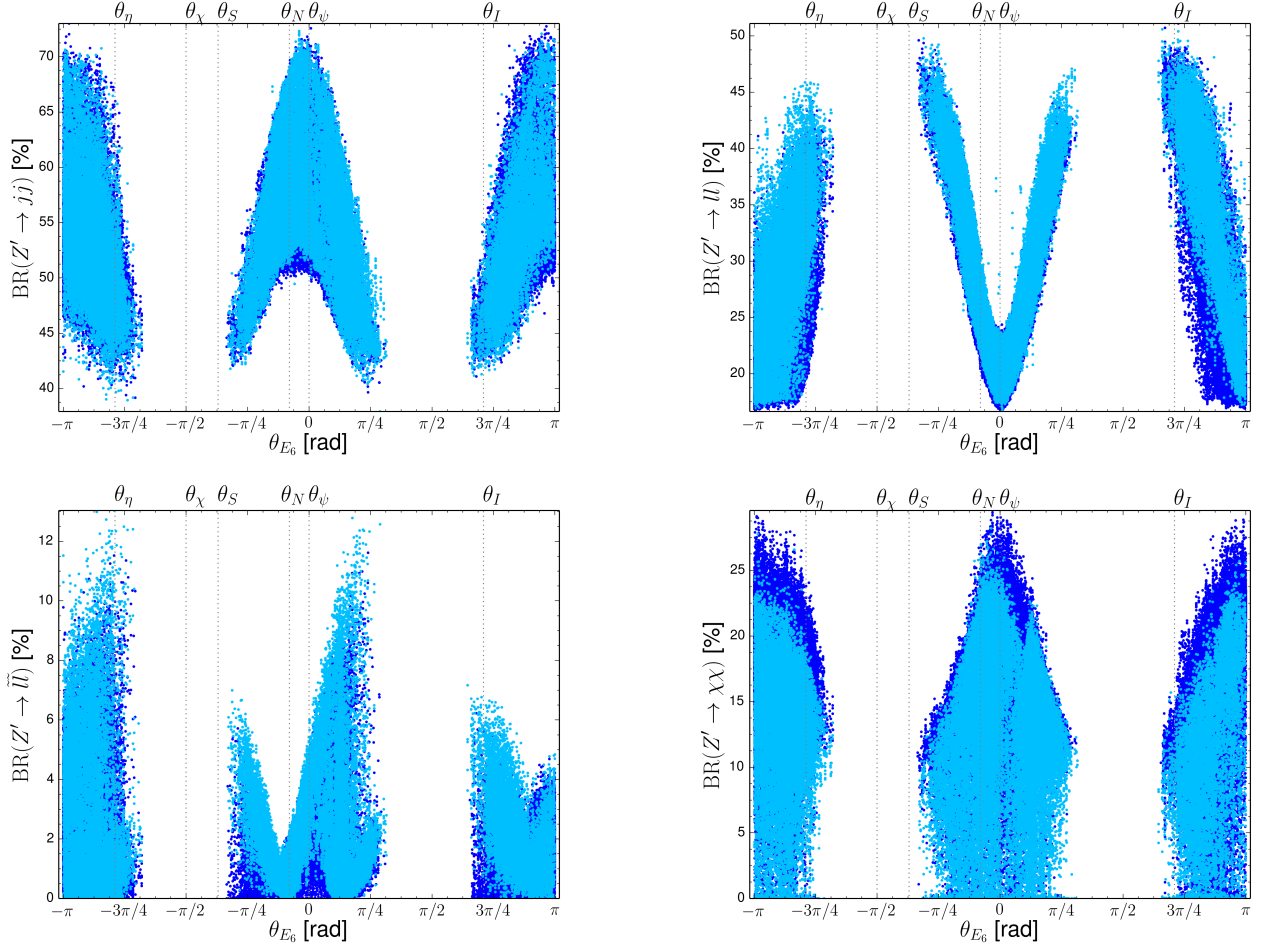


FIG. 4: Same as in Fig. 2 but for the branching ratios of the  $Z'$  boson for several decay channels, namely the  $Z'$  decays into a pair of jets (upper left), a pair of leptons (upper right), a pair of sleptons (lower left) and a pair of neutralinos or charginos (lower right).

### 3.3. $Z'$ phenomenology

Typical  $Z'$  phenomenology can be dramatically different in the presence of supersymmetry, in particular due to the existence of new  $Z'$  decay channels into pairs of SUSY particles. This is illustrated in Fig. 4 where we analyse different options for the  $Z'$  decays as a function of the mixing angle  $\theta_{E_6}$ .

Our results show that there is very little hope to be able to use  $Z'$  decay rates to differentiate  $U(1)'$  models. Decays into slepton pairs are consistently small, while leptonic channels, that are also present in non-supersymmetric cases, exhibit branching ratios ranging from 0 to about 50%. A leptophobic behaviour emerges for specific mixing angles, but these features can be reproduced for other realisations where a large leptonic  $Z'$  branching fraction is as well common. This nevertheless leads to one of the most promising channels to look for a sign of  $U(1)'$  new physics, by bump hunting in the dilepton mass distribution for LHC events featuring two opposite-sign final state leptons, provided the branching is large enough. The same conclusion holds for the dijet decay mode that corresponds to the preferred  $Z'$  decay mode, regardless of the value of  $\theta_{E_6}$ . The only limiting factor is, both for the dilepton and dijet case, the  $Z'$  mass driving the production cross section and the associated phase space suppression in the heavy case.

In the lower right panel of the figure, we investigate the magnitude of the  $Z'$  branching fraction into a pair of neutralinos or charginos. Such decays can often be abundant, with a branching ratio reaching about 20%, and yield a  $Z'$  signature made of both leptons and missing energy. This potentially allows for the distinction of SUSY and non-SUSY  $Z'$ -bosons.

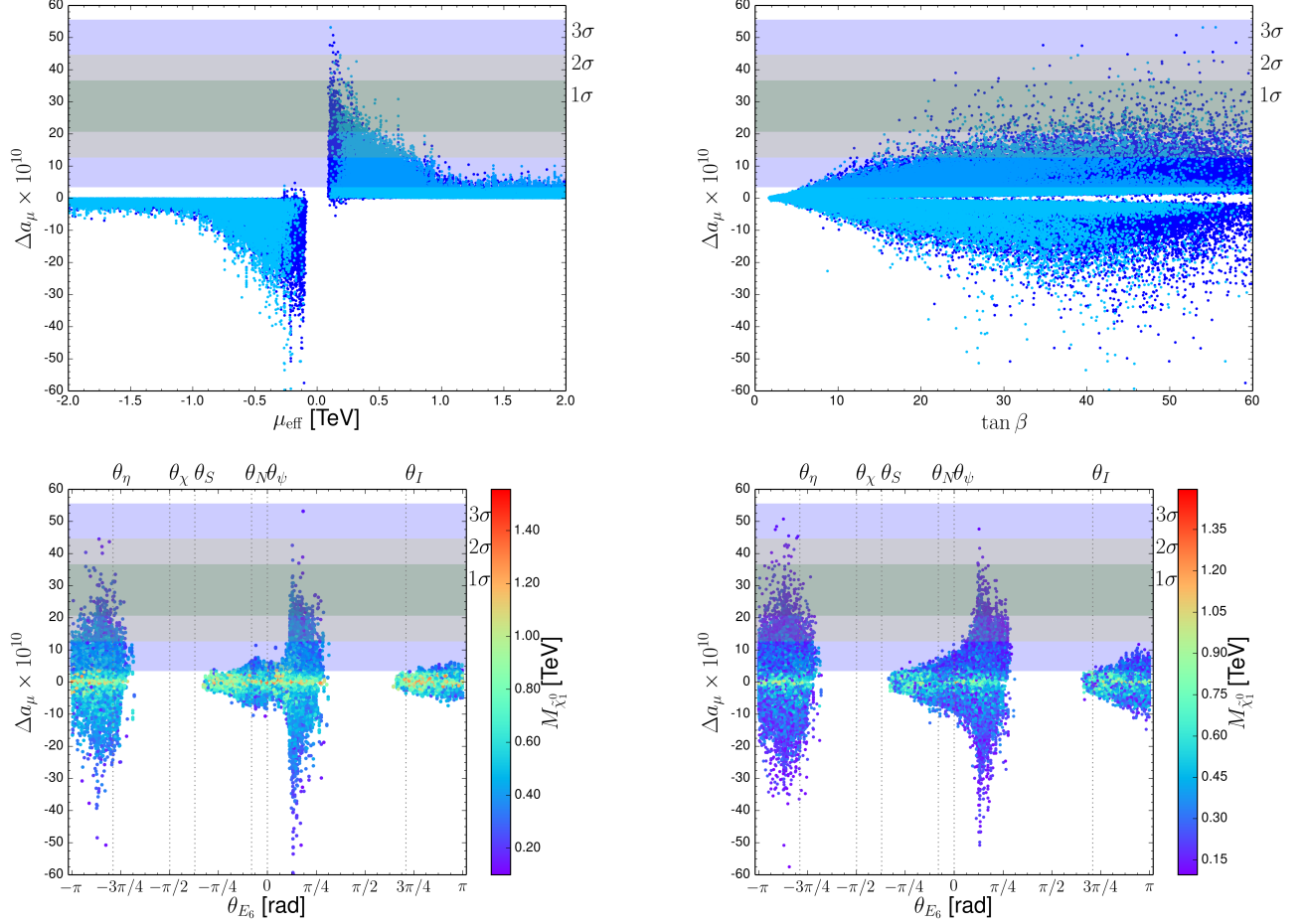


FIG. 5: *UMSSM contributions to the anomalous magnetic moment of the muon,  $\Delta a_\mu$  shown as a function of the effective  $\mu_{\text{eff}}$  parameter (upper left) and  $\tan \beta$  (upper right). The light (dark) blue points represent scenarios in which the lightest sneutrino (neutralino) is the LSP. On the lower panels of the figure, we present the  $\theta_{E_6}$  dependence of  $\Delta a_\mu$  and depict by a colour code the mass of the lightest neutralino for scenarios with a sneutrino (lower left panel) and with a neutralino (lower right panel) LSP. On all figures, we moreover indicate by a green, grey and purple band the  $\Delta a_\mu$  values for which we get an agreement at the  $1\sigma$ ,  $2\sigma$  and  $3\sigma$  level with the experimental value, respectively.*

### 3.4. The anomalous magnetic moment of the muon

Pioneering results from the BNL E821 experiment [67], their improvements at the FNAL E989 experiment [68] and the anticipated results obtained from the J-PARC E34 experiment [69] have provided a very precise measurement of the anomalous magnetic moment of the muon  $(g-2)_\mu$ . The measured value departs by about  $3\sigma$  from the SM expectation,

$$a_\mu^{\text{SM}} = 116591828(2)(43)(26) \times 10^{-11}, \quad (3.2)$$

which constitutes a challenge for beyond the SM model building. In the UMSSM framework, both the presence of the extra gauge boson and a neutral and charged (s)lepton sector in the presence of a sneutrino or neutralino LSP can have a drastic impact on the anomalous magnetic moment of the muon via loop-induced contributions. As the LSP is often much lighter than the  $Z'$  boson, the corresponding SUSY contributions are expected to be more important than any additional  $Z'$  contribution. As in the MSSM, new physics effects on  $(g-2)_\mu$  are therefore mostly depending on  $\tan \beta$  and the effective  $\mu_{\text{eff}}$  parameter, which determine the higgsino masses and the fermion and sfermion interactions with the higgs(ino) sector.

For each point of our parameter space scan, we present in the upper panel of Fig. 5 the UMSSM contributions to  $(g-2)_\mu$ , that we denote by  $\Delta a_\mu$ , and that is expected to fill the gap between the theoretical predictions and  $(g-2)_\mu$  data. The dependence of  $\Delta a_\mu$  on the  $\mu_{\text{eff}}$  parameter is depicted on the left panel of the figure, and we observe that



the gap between the experimental measurement and the theoretical prediction can only be filled for positive value of  $\mu_{\text{eff}}$ . As in the MSSM, this originates from neutralino and slepton loop contributions that are proportional to  $\mu_{\text{eff}}$ , so that a negative  $\mu_{\text{eff}}$  value would increase and not decrease the discrepancy between theory and experiment. Sneutrino LSP scenarios mostly feature a small  $\mu_{\text{eff}}$  value, as already found in Fig 2, which implies that the lightest neutralino is in general not too heavy. As a consequence, the corresponding contributions to  $(g-2)_\mu$  are sizable and theoretical predictions agree better with data (for cases where  $\mu_{\text{eff}} > 0$ ). This agreement is in addition facilitated for large  $\tan\beta$  values, as shown in the right panel of the figure. Neutralino LSP scenarios in contrast allow for intermediate  $\mu_{\text{eff}}$  values, so that resulting  $\Delta a_\mu$  new physics contributions are not large enough to entirely fill the experiment-theory gap due to a heavy neutralino mass suppression.

These conclusions are further confirmed by the lower panel of Fig. 5 in which we show the variation of  $\Delta a_\mu$  as a function of the  $U(1)'$  mixing angle  $\theta_{E_6}$  and correlate the results with the value of the mass of the lightest neutralino for sneutrino LSP scenarios (left panel) and neutralino LSP scenarios (right panel). We observe that in contrast to the other models,  $U(1)_I'$  scenarios are unable to provide an explanation for the  $(g-2)_\mu$  observations. This is connected to the larger  $M_{1/2}$  mass parameter typical of these scenarios. The contributions from  $U(1)'$  supersymmetric models to  $\Delta a_\mu$  are dominated by slepton-neutralino loop diagrams, and are maximal for light sleptons. This occurs when the  $D$ -terms proportional to  $Q_l$  in the slepton mass matrix are zero as in Fig. 1, which corresponds to the peaks appearing in the lower panel graphs of Fig. 5.

#### 4. SNEUTRINO DARK MATTER

In this section we concentrate on scenarios exhibiting a sneutrino LSP and show that sneutrinos are UMSSM viable dark matter candidates, in contrast to the MSSM possibly extended with right sneutrinos. Unlike in a theory featuring only the SM gauge group, right sneutrinos can reach, in the UMSSM, thermal equilibrium thanks to their  $U(1)'$  interactions with extra vector and/or scalar fields. Moreover, the sneutrino pair annihilation cross section is possibly enhanced by  $s$ -channel resonant (or near-resonant) exchanges, and the elastic scattering cross section of a dark matter particle with a SM parton is suppressed by several orders of magnitude as sneutrino couplings to the SM  $Z$  and Higgs bosons are reduced and the would-be dominant  $Z'$  exchange is mass-suppressed.

Our thorough investigation of the MSSM parameter space has revealed that, when allowing the model parameters to be small and run freely, the lightest neutralino naturally emerges as the LSP. Requiring a sneutrino to be the LSP implies more specific and less general corners of the parameter space, which is not necessarily an issue as the absence of any beyond the SM signal at the LHC could be an indication for a non-natural new physics setup. We now focus on the dark matter implications for all scanned scenarios exhibiting a sneutrino LSP in the  $U(1)'_\psi$ ,  $U(1)'_\eta$  and  $U(1)'_I$  models, that are the three-anomaly free UMSSM setups satisfying so far all current constraints, and investigate constraints originating from the dark matter relic abundance in Sec. 4.1 and direct detection and neutrino fluxes in Sec. 4.2.

##### 4.1. Relic Density

In order to analyse the constraints that could originate from the relic density on the UMSSM models, we explicitly choose two possibilities for the  $Z'$ -boson mass, a light  $Z'$ -boson case with  $M_{Z'} = 2$  TeV and a heavier  $Z'$ -boson case with  $M_{Z'} = 2.5$  TeV. Although the former option is slightly less than the  $Z'$ -boson limits presented in the 2016 Particle Data Group review [59], we recall that such light extra bosons are allowed in UMSSM scenarios where  $Z'$  decays into pairs of supersymmetric particles contribute significantly. Moreover, we use the results of our scan to enforce the values for other parameters to lead to a viable Higgs boson mass and a fair agreement with all other experiment constraints. The relic density contributions stemming from the presence of a  $Z'$  boson are crucial for models such as the UMSSM where the field content of the theory includes right sneutrinos that are not sensitive to the SM gauge interactions. Whilst a full parameter space scan could be in order, the above procedure allows us to study and understand the impact of specific parameters on the relic density, and in particular of the effective  $\mu_{\text{eff}}$  parameter and the trilinear coupling  $A_\lambda$ , as in general, sneutrino DM is usually overabundant as a result of an inefficient sneutrino annihilation mechanism. We use as experimental bounds for the relic density the conservative range provided from the older WMAP data [70, 71] and including a 20% uncertainty,

$$\Omega_{\text{DM}} h^2 = 0.111^{+0.011}_{-0.015}. \quad (4.1)$$

Fixing first  $M_{Z'}$  to 2 TeV, we investigate the dependence of the relic density on the mass of the lightest sneutrino, after selecting varied choices of  $M_{\tilde{\chi}_1^0}$ ,  $\mu_{\text{eff}}$  and  $A_\lambda$ . In addition, the  $\tan\beta$ ,  $M_0$  and  $A_0$  parameters are modified

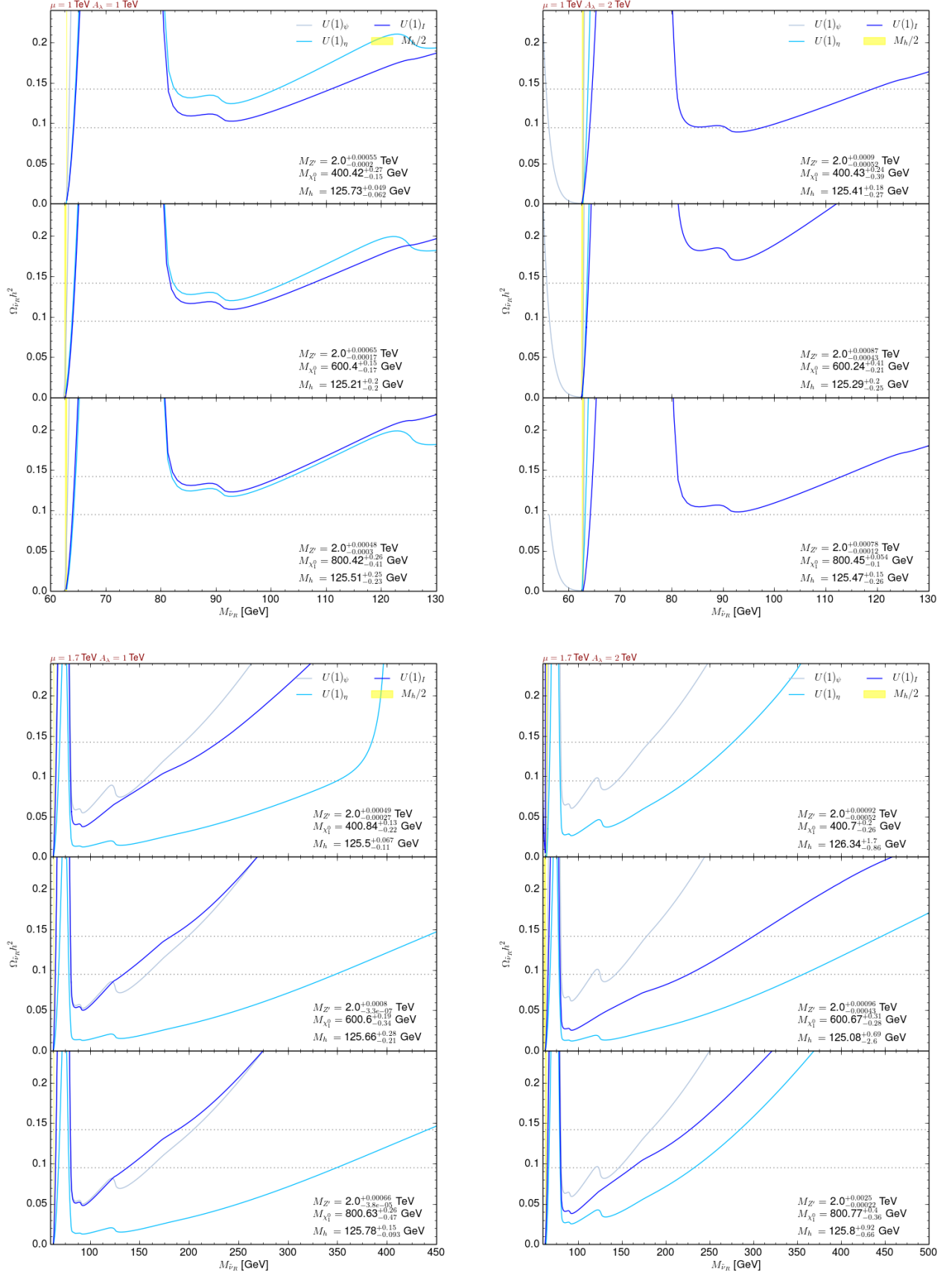


FIG. 6: Dependence of the relic density for UMSSM scenarios featuring a right sneutrino LSP and  $M_{Z'} = 2 \text{ TeV}$ . We fix  $\mu_{\text{eff}}$  to 1 TeV (upper panels) and 1.7 TeV (lower panels), as well as  $A_\lambda$  to 1 TeV (left panels) and 2 TeV (right panels). In each of the four figures, the lightest neutralino mass has been respectively fixed to 400 GeV (upper inset), 600 GeV (middle inset) and 800 GeV (lower inset) and we focus on the  $U(1)'_\psi$  (grey),  $U(1)'_\eta$  (light blue) and  $U(1)'_I$  (dark blue) models.

correspondingly to recover a correct lightest Higgs boson mass of 125 GeV, and agreement with all the previously discussed experimental constraints. We consider, in our analysis, three parameter space regions on the basis of the mass of the lightest neutralino, which is most often the next-to-lightest superpartner (NLSP), here taken to be 400 GeV, 600 GeV and 800 GeV respectively. Alongside the neutralino mass,  $\mu_{\text{eff}}$  and  $A_\lambda$  are set to 1 or 1.7 TeV and 1 or 2 TeV respectively, this restricted set of values being sufficient to investigate the effects on these parameters on the dark matter relic density. The results are presented in Fig. 6.

In the upper right panel of the figure, we set  $\mu_{\text{eff}} = A_\lambda = 1$  TeV and show that regardless of the value of the lightest neutralino mass and depending on the class of  $U(1)'$  model, there exist two regimes where the predicted relic density matches the observations. First, in a region where the sneutrino mass is close to 65 GeV, one can design  $U(1)'_\eta$ ,  $U(1)'_\psi$  and  $U(1)'_I$  UMSSM models where the relic density bounds are satisfied. A correct dark matter annihilation cross section can be achieved thanks to the enhanced contributions of Higgs-boson exchange diagrams that proceed in a resonant or near-resonant production mode ( $M_{\tilde{\nu}_1} \approx M_h/2$ ). This configuration, also known as a Higgs funnel configuration, is achievable for any value of the  $\mu_{\text{eff}}$  and  $A_\lambda$  parameters, as shown in the other panels of Fig. 6, although the value of  $A_\lambda$  affects its size. The Higgs funnel region is indeed narrower for larger  $A_\lambda$  values. While a similar regime could be expected for  $M_{\tilde{\nu}_1} \approx M_{Z'}/2$ , this latter setup implies very heavy sneutrinos that are then incompatible with the requirement of a sneutrino being the LSP.

A second kinematical regime allows for the recovery of a proper relic density, with a sneutrino mass lying in the [80, 110] GeV window for  $\mu_{\text{eff}} = A_\lambda = 1$  TeV (upper left panel of the figure). In this regime, both dark matter annihilation into a pair of  $Z$ -bosons and LSP-NLSP co-annihilations are important, as noticed by the size of the region depending on the mass of the lightest neutralino. Investigating the other panels of the figure, one observes that the exact details of this region of the parameter space, as well as its existence, strongly depend on the values of the  $\mu_{\text{eff}}$  and  $A_\lambda$  parameters. The latter indeed directly affect the nature of the lightest neutralino and the properties of the heavier part of the Higgs sector,  $h_1$  exchange contributions being very relevant for a not too heavy next-to-lightest Higgs boson (see Fig. 3).

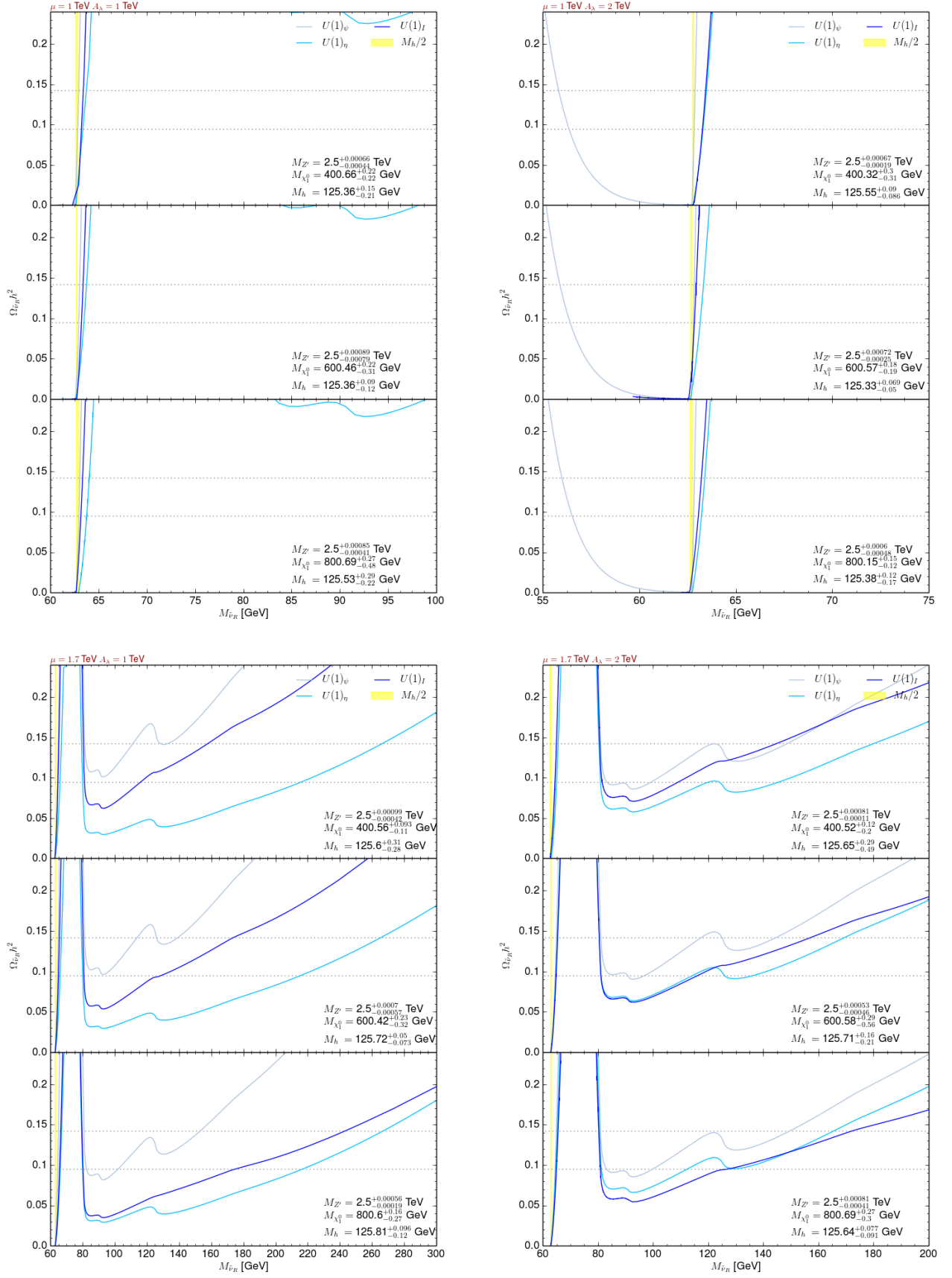
$Z'$ -boson exchange contributions play nevertheless a key role in the calculation of the relic density. For instance, in  $U(1)'_\psi$  scenarios, the new gauge interactions of the sneutrinos are relatively weaker (due to the involved  $U(1)'$  charges), the corresponding branching ratio being three times smaller than for the two other cases. As a result, the existence of the heavier sneutrino regime itself, in which the relic density constraints are correctly satisfied, is more challenging. This feature is emphasised on Fig. 7 where the  $Z'$ -boson mass is pushed to 2.5 TeV, the other  $M_{\tilde{\chi}_1^0}$ ,  $A_\lambda$  and  $\mu_{\text{eff}}$  parameters being varied as before whereas the  $\tan\beta$ ,  $M_0$  and  $A_0$  parameters are once again adjusted to reproduce all previously considered constraints. Although the existence of the Higgs funnel regime is barely affected by the changes, this regime may be shifted towards lighter sneutrino masses in the [50, 65] GeV regime. In addition, heavier sneutrino LSP scenarios are more difficult to accommodate, which directly prevents the heavy sneutrino regime with a consistent relic density from existing, in particular if the  $\mu_{\text{eff}}$  parameter is not large enough.

#### 4.2. Constraints from dark matter direct detection and neutrino fluxes

Direct detection experiments aim to detect DM scattering off nuclear matter and to measure its properties. While the DM interactions with nuclear matter can be generally classified as spin-dependent or spin-independent, only the latter is relevant for sneutrino dark matter. We present, in Fig. 8, UMSSM predictions for the spin-independent cross section associated with the scattering the LSP with protons (left panel) and neutrons (right panel), and compare them with the experimental results from the LUX experiment [72]. We adopt UMSSM scenarios in which  $\mu_{\text{eff}} = 1.7$  TeV and  $A_\lambda = 2$  TeV, and the  $Z'$  mass is fixed to 2.5 TeV. As in the previous section, the results are given for lightest neutralino masses of 400 GeV (top inset), 600 GeV (central inset) and 800 GeV (lower inset).

Our results demonstrate the discriminating power of the spin-independent DM-nucleon scattering cross section as its behaviour as a function of the mass of the sneutrino LSP highly depends on the  $U(1)'$  model. For a given LSP mass, cross section values obtained in  $U(1)'_I$  models are one order of magnitude larger than for the two other classes of models,  $U(1)'_\eta$  cross sections increasing in addition with the sneutrino mass. The results of the LUX experiment introduce strong constraints on wide regions of the parameter space, and our specific  $\mu_{\text{eff}}$  and  $A_\lambda$  choice are typical from the parameter space region in which both the relic density and the direct detection constraints can be easily accommodated. This however introduces tensions with the parameter space regions favoured by the anomalous magnetic moment of the muon results (see Sec. 3.4), and only the Higgs funnel region in which the sneutrino mass is half of the Higgs-boson mass survives to all constraints.

While  $U(1)'_I$  models are clearly disfavoured by direct detection data,  $U(1)'_\psi$  scenarios cannot feature a viable light sneutrino DM, whilst  $U(1)'_\eta$  setups in contrast prefer light LSP configurations with a sneutrino mass of about 60 GeV to 100 GeV depending on the neutralino mass. These results stem from the interaction of the lightest sneutrino with the  $Z$ ,  $Z'$  and Higgs bosons. As the lightest sneutrino only very weakly couples to the SM sector, the scattering cross

FIG. 7: Same as in Fig. 6 but for  $M_{Z'} = 2.5$  TeV.

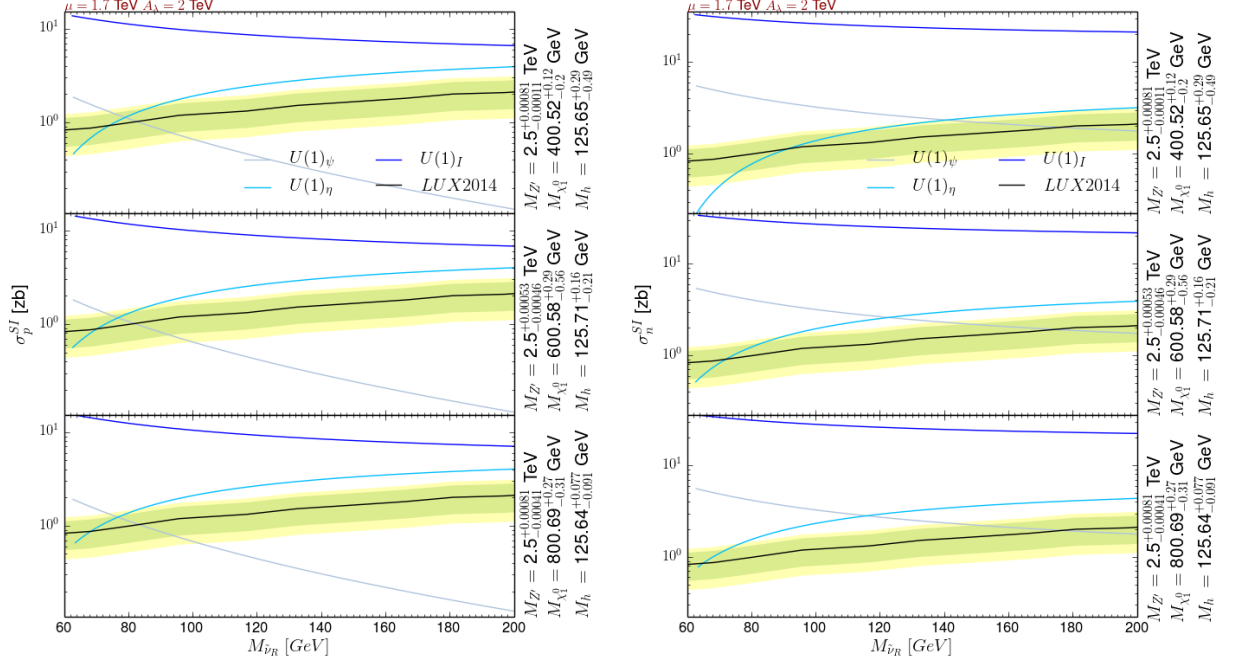


FIG. 8: Spin independent cross section associated with the scattering of dark matter off protons (left) and neutrons (right) presented as functions of the dark matter mass. We fix  $\mu_{\text{eff}}$  to 1.7 TeV and  $A_\lambda$  to 2 TeV. In each of the subfigures, the lightest neutralino mass has been respectively fixed to 400 GeV (upper inset), 600 GeV (middle inset) and 800 GeV (lower inset) and we focus on the  $U(1)_\psi$  (grey),  $U(1)_\eta$  (light blue) and  $U(1)_I$  (dark blue) models. The band corresponds to the  $2\sigma$  limits extracted from LUX data [72, 73].

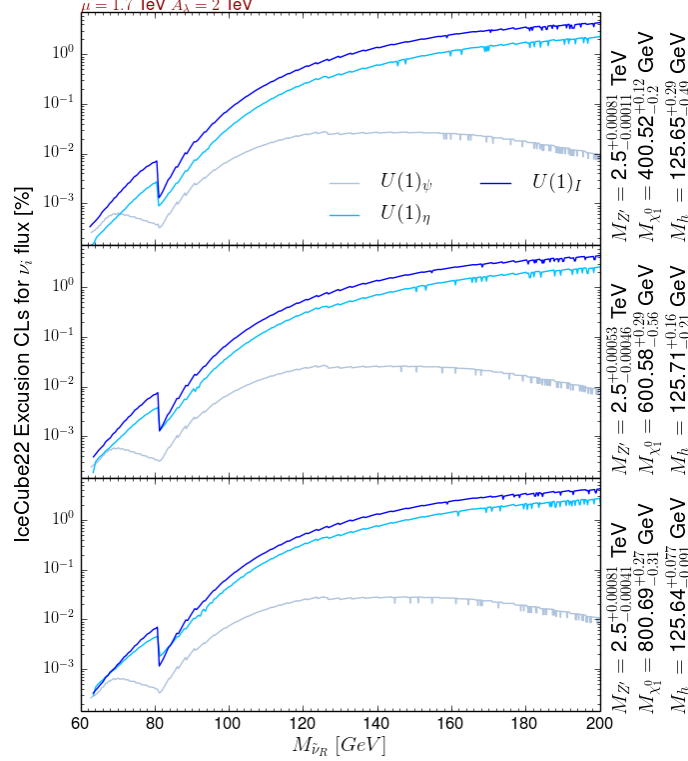


FIG. 9: Exclusion bounds, given as a confidence level, extracted from the neutrino flux observed in the IceCube experiment and presented as a function of the lightest sneutrino mass. The UMSSM scenario is fixed as in Fig. 8.



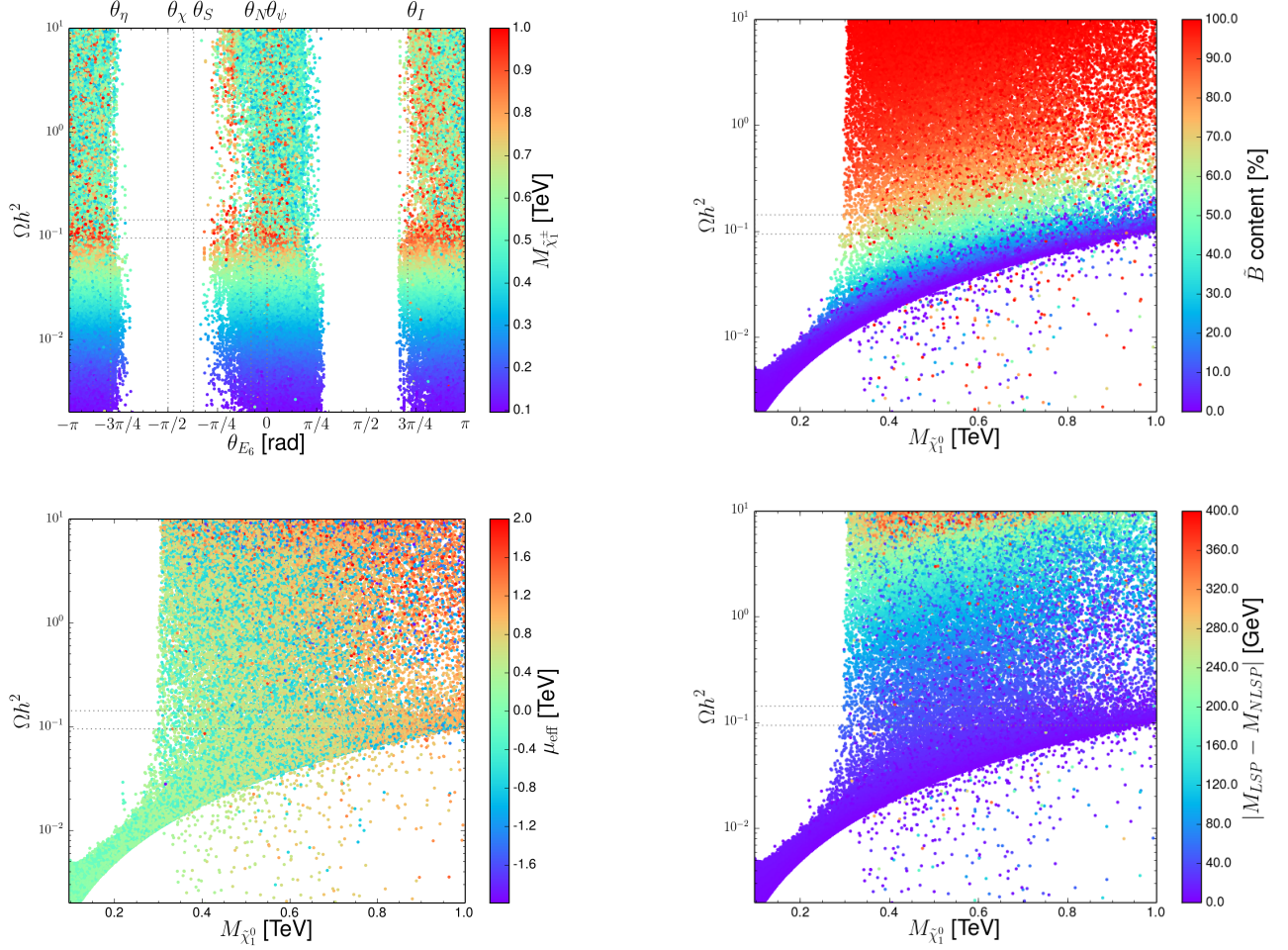


FIG. 10: DM relic density obtained for UMSSM scenarios featuring a neutralino LSP, presented as a function of the LSP mass and the  $U(1)'$  mixing angle (upper left panel), the neutralino bino component (upper right panel), the  $\mu_{\text{eff}}$  parameter (lower left panel) and the mass difference between the LSP and the NLSP (lower right panel).

section mostly depends on the vectorial couplings of the LSP and of the SM quarks to the  $Z'$ -boson. These quark vectorial couplings being vanishing in the  $U(1)_{\psi}$  model, the resulting cross section is largely suppressed and those scenarios can survive more easily to LUX data. The neutron cross section, being larger as expected [27], however drastically reduces the size of the allowed region of the parameter space and future improvements in direct detection experiments may directly challenge the studied UMSSM setups.

Recent observations of ultra-high energy neutrino events at the IceCube experiment [74] indicate a possible deficit in the amount of observed muon tracks, which is known as the muon deficit problem, and an apparent energy gap in the three-year high energy neutrino data. This challenges any explanation based on atmospheric neutrinos, and suggests an extra-terrestrial origin that could involve dark matter. Data being however consistent with the SM expectation, this may introduce extra constraints when DM model building is at stake. We present, in Fig. 9, the corresponding exclusion as obtained in the UMSSM setup considered in this section with the help of MICROMEGAS. This shows that even if genuine differences amongst the three considered  $U(1)'$  options once again appear, in particular for large sneutrino masses, all results are consistent with the SM to a good extent.

## 5. NEUTRALINO DARK MATTER

As shown in the above sections, the LSP can naturally be the lightest neutralino, that consists in UMSSM scenarios of an admixture of  $\lambda_{\tilde{B}}$ ,  $\lambda_{\tilde{W}}$  and  $\lambda_{\tilde{Z}'}$  gauginos, as well as of higgsinos. Whether the LSP in a particular setup is able to yield the right relic abundance depends crucially on its composition. For a bino-dominated or a bino'-dominated

neutralino, the LSP is a gauge singlet and it annihilates mainly through sfermion  $t$ -channel exchanges. As sfermions are heavy, the annihilation mechanism is often inefficient so that accommodating the observed relic density is difficult, unless one strongly relies on co-annihilations. The relic density can be more easily reproduced when the lightest neutralino is of a higgsino or wino nature, or a mixed state. If the LSP is higgsino-like, its mass is driven by the  $\mu_{\text{eff}}$  parameter, as is the mass of the lightest chargino and of the next-to-lightest neutralino. These three particles being almost degenerate, annihilations and co-annihilations easily occur so that DM could be underabundant if the LSP is too light [75]. In our setup the wino-like LSP is in contrast impossible to be realised due to the GUT relations that we have imposed in our scanning procedure.

Unlike for sneutrinos, the neutralino LSP mass is mainly determined by the  $M_{1/2}$  and the  $\mu_{\text{eff}}$  parameters that also affect *all* the particle masses of the model. The LSP mass cannot be consequently varied independently of the rest of the spectrum, making an analysis based on specific benchmark configurations less straightforward than in the sneutrino LSP case. We therefore base our study on the results of our parameter space scan where all the constraints described in Sec. 3.1 are imposed. Our results are given in Fig. 10 where we present the dependence of the DM relic density on the LSP mass. We correlate our findings with the value of the  $U(1)'$  mixing angle  $\theta_{E_6}$  (upper left panel), the magnitude of the LSP bino component (upper right panel), the value of the  $\mu_{\text{eff}}$  parameter (lower left panel) and the mass difference between the LSP and the NLSP (lower right panel). Accommodating the correct relic density yields a LSP mass of at least 300 GeV, which contrasts with sneutrino LSP scenarios where the mass of the latter is smaller. As expected, the lightest neutralino is mostly bino-like, and a higgsino component is only allowed for heavier LSP setups so that the co-annihilation rate turns out to be tamed. Viable DM scenarios also feature a small  $\mu_{\text{eff}}$  parameter lying in the  $[-400, 400]$  GeV mass window, which allows the next-to-lightest neutralino to be higgsino-like and not too heavy, as emphasised in the lower right panel of the figure as it is often the NLSP. Co-annihilations are hence under good control, which guarantees a relic density in agreement with the observations. Our results also show that small differences are present for the different  $U(1)'$  scenarios under consideration, the LSP mass being only in general slightly larger for  $U(1)_I'$  models.

In Fig. 11, we include constraints that arise from DM direct detection experiments and correlate the proton-DM (upper left panel) and neutron-DM (upper right panel) spin-independent scattering cross section with the predicted relic density, including in addition information on the LSP mass for each point. This shows, together with the results of the lower right panel of the figure, that regardless of the LSP mass, there are always scenarios for which both the relic density and the direct detection constraints can be satisfied. We finally correlate, in the lower left panel of the figure, the relic density and the confidence level exclusion that can be obtained from the IceCube results on the neutrino flux. We observe that contrary to the sneutrino LSP case, here neutrino flux results play a role in constraining the UMSSM parameter space.

## 6. COLLIDER SIGNALS

New physics models featuring a dark matter candidate can in general be equally tested with cosmology and collider probes and extra pieces of information can be obtained when both sources of constraints are considered in complementarily [76]. In the previous sections, we have discussed the DM phenomenology of UMSSM realisations in which the LSP is either the lightest sneutrino or the lightest neutralino, with the hope of getting handles allowing for the distinction of the gauge group structure. In this section, we focus on the potential searches that could be performed at the LHC, in particular when a part of the particle spectrum is light and when the high-luminosity LHC run is considered. To determine the signals to be searched for, we focus on a set of promising benchmarks obtained from our scan results for which all constraints are satisfied. This in particular concerns scenarios featuring a light sneutrino LSP. In order to evaluate the fiducial cross sections associated with various signals, we export the UMSSM to the UFO format [77] and make use of the MG5\_aMC@NLO framework version 2.4.3 [78] to simulate hard-scattering LHC collisions. The QCD environment characteristic of hadronic collisions is simulated by means of the Pythia 8 program version 8.2.19 [79] and we rely on the Delphes 3 package version 3.3.2 [80] for the modelling of the response of a typical LHC detector. The resulting detector-level events are reconstructed by using the anti- $k_T$  jet algorithm [81] as embedded in the FastJet library version 3.1.3 [82], and the reconstructed events are analysed within the MadAnalysis 5 framework version 1.4.18 [83].

The best studied DM signatures at the LHC consist of the mono- $X$  probes for which a certain amount of missing transverse energy (carried by one or more DM particles) is produced in association with a single energetic visible SM object. As in the case of other models, monojet signals are thought as the most promising due to the relative magnitude of the strong coupling with respect to the other gauge couplings. The corresponding rates are however very reduced in the case of a sneutrino LSP, in particular once one imposes a typical monojet selection that requires the presence of a jet with a large transverse momentum and a veto on final state leptons. Additionally, dark matter can also be produced together with an electroweak vector boson or a  $Z'$  boson radiated off the initial state. While

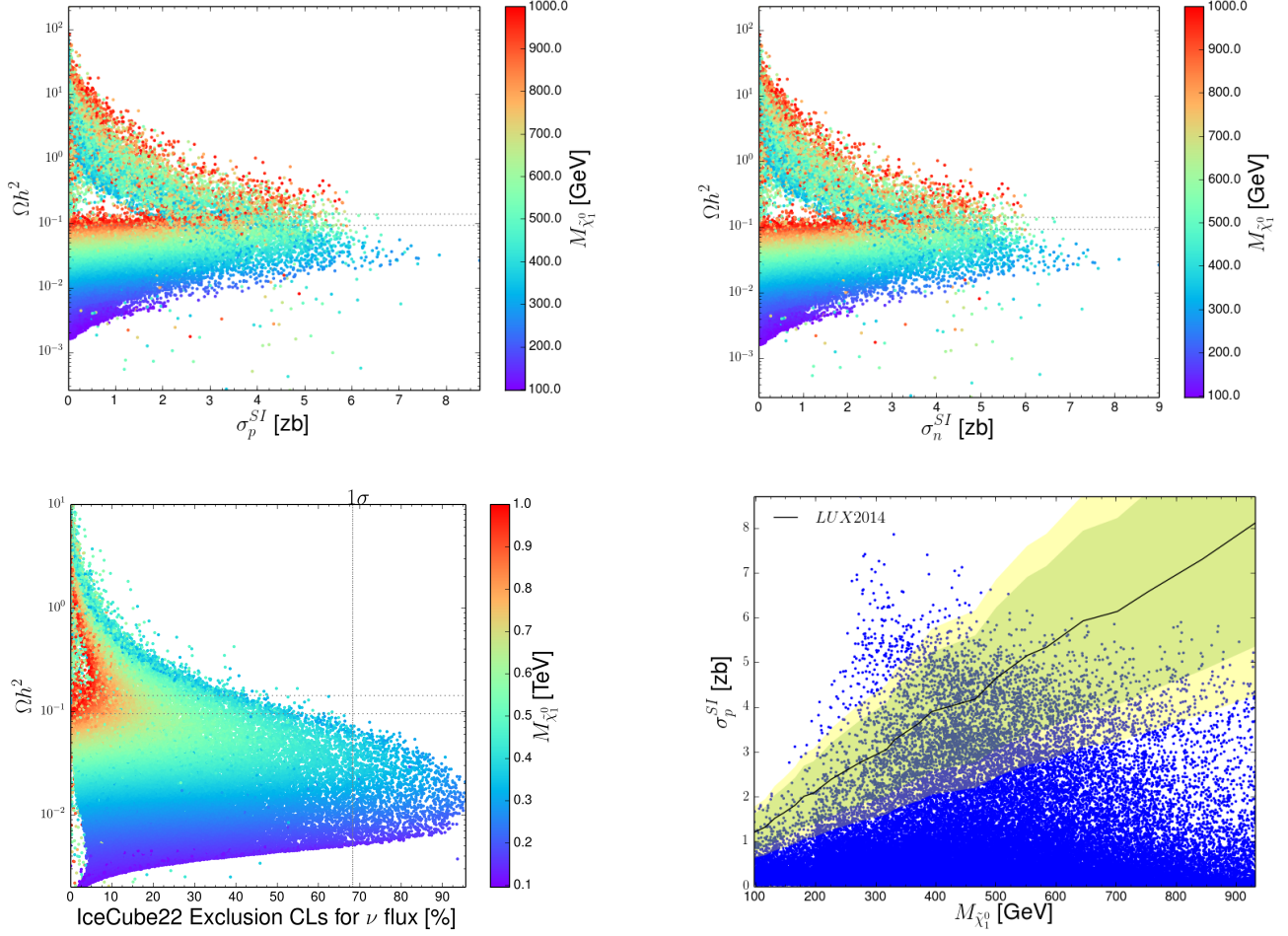


FIG. 11: Constraints on the UMSSM parameter space region in which the LSP is a neutralino that originate from DM direct detection. We present the dependence of the relic density on the neutralino mass and on the resulting spin-independent dark matter scattering cross section with protons (upper left panel) and neutrons (upper right panel) and on the possible exclusion that could be obtained from IceCube results (lower left panel). We also show the dependence of the spin-independent DM-proton scattering cross section on the neutralino mass, including the bound stemming from the LUX experiment (lower right panel).

the corresponding production cross section is expected to be smaller than the monojet one, the final state offers more freedom to reject the background and is thus worthy to be searched for. Moreover, if as in the UMSSM case, DM particles strongly couple to SM or extra gauge bosons, mono-vector boson production may be the dominant channel yielding DM production at the LHC. However, once all the constraints considered in the previous section are imposed, the remaining regions of the parameter space correspond to cross sections that are either negligible or too small relatively to the background cross sections.

Another way to probe phenomenologically viable UMSSM scenarios is to focus on sfermion pair production, and in particular on the production of the lighter third generation sfermions. The considered UMSSM scenarios feature heavy stops and sbottoms, so that third generation squark pair-production could be in principle easily tagged thanks to the subsequent presence of very hard final state objects. However, the associated production total rates are of the order of at most 1 fb. This makes any new physics contribution impossible to observe relative to the overwhelming SM background, even if advanced analysis techniques relying on the shape of the differential distributions are used. Moving on with the slepton sector, stau pair production is not expected to offer any extra handle on UMSSM-induced new physics, as the related rates are suppressed due to the electroweak nature of the process. The possible enhancement arising from the  $Z'$  contributions is in addition reduced given the low  $Z'$ -bosons branching ratios into sleptons (see Fig. 4).

Finally, we have studied chargino and neutralino pair-production, and in particular the associated production of one chargino and one neutralino that could be enhanced when the effective  $\mu_{\text{eff}}$  parameter is small [84]. The subsequent

associated signatures can contain one, two or more than two leptons, jets and missing energy. Fiducial cross sections of the order of the fb are obtained, which are nonetheless too small to be distinguished from the SM background even after relying on a judicious selection strategy.

The challenges of observing viable UMSSM models at colliders are not unique, and it turns out that scenarios that are in principle observable at colliders are disfavoured by cosmology, and that scenarios in agreement with cosmological and astrophysical data are out of reach of any present collider.

## 7. SUMMARY AND CONCLUSION

We have presented an extensive phenomenological exploration of  $U(1)'$  supersymmetric models that can be classified according to the way a grand unified  $E_6$  symmetry would be broken. Our study has revealed that a large volume of the parameter space is compatible with constraints originating from cosmology, astrophysics, precision tests, Higgs physics at the LHC, but that these constraints have simultaneously a significant impact on the determination of the favoured regions of the parameter space. As allowed scenarios can equally feature the lightest sneutrino or the lightest neutralino as dark matter candidates, we have investigated the existence of handles to differentiate between these two options in the context of the five anomaly-free  $U(1)'$  setups. We have scanned the UMSSM parameter space for phenomenologically viable models, imposing unification conditions at the GUT scale and allowing the remaining parameters to run freely. While sneutrino LSP is possible only in  $U(1)'_\psi$ ,  $U(1)'_\eta$  and  $U(1)'_I$  models,  $U(1)'_N$  setups have the particularity that right sneutrinos decouple from the  $U(1)'$  sector so that only a neutralino LSP can be a viable dark matter candidate. In addition, anomaly-free  $U(1)'_\chi$  and  $U(1)'_S$  realisations cannot induce a viable symmetry breaking pattern due to the  $U(1)'$  charge assignments and are thus excluded.

We have additionally found that in general the neutralino emerges as the most natural LSP, but that sneutrino LSP scenarios are possible when the corresponding soft masses are small, which is possible as they are independent of the other parameters. In particular, the parameter space region consistently preferred by the cosmology is when  $M_{\tilde{\nu}_1} \simeq M_h/2$ . This inhabits the so-called Higgs-funnel regime where the observed relic density can be accommodated thanks to the contributions of resonant Higgs exchange diagrams. All direct detection bounds can additionally be satisfied, and an explanation for anomalous magnetic moment of the muon data can be proposed for  $U(1)'_\eta$  and  $U(1)'_\psi$  models, all other  $U(1)'$  models being unable to fulfill all constraints at the same time. Depending on other parameter values, higher sneutrino mass regions can open up, but such regions are limited by other dark matter constraints. For the considered benchmark scenarios, this includes  $U(1)'_\psi$  models where the sneutrino mass lies in the 80-140 GeV range. The situation is slightly better for neutralino LSP scenarios, where several other viable  $U(1)'$  choices exist. The LSP mass in these cases can either be small, when the neutralino LSP is mainly bino-like, or much larger, when the neutralino LSP has a large or dominant higgsino component and is close in mass to the NLSP. This last configuration allows an appropriate amount of co-annihilations with the NLSP and consequently avoids any tension with the cosmological data. We have moreover observed that in sneutrino LSP scenarios, the second lightest Higgs boson is likely degenerate in mass with the  $Z'$  boson for  $U(1)'_\eta$  and  $U(1)'_\psi$  models, which consists of an indication that it is mostly singlet. In contrast,  $U(1)'_I$  scenarios favour a lighter second Higgs boson with a larger doublet component.

Unfortunately these UMSSM scenarios do not have good prospects for observability in present collider experiments, even when the high-luminosity run of the LHC is considered. All signal cross sections are too small and the background is thus overwhelming for all the possible associated new physics signatures. Our predictions for the spin-independent cross section related to DM direct detection are nonetheless within the reach of the future of XENON-1T experiment [85], that is expected to be sensitive to cross section values of about  $1.6 \times 10^{-47} \text{ cm}^2$  for DM masses of 50-60 GeV. This should allow for conclusive statements regarding the viability of any of the UMSSM scenarios presented in this work.

## Acknowledgments

The authors thank Gennaro Corcella and Florian Staub for their help with the usage of the SARAH program, as well as Olivier Mattelaer and Torbjörn Sjöstrand for their help with MADGRAPH5\_AMC@NLO and PYTHIA8. MF acknowledges NSERC for partial financial support under grant number SAP105354. The work of BF is partly supported by French state funds managed by the Agence Nationale de la Recherche (ANR), in the context of the



- 
- [1] ATLAS collaboration, *Search for pair production of gluinos decaying via top or bottom squarks in events with b-jets and large missing transverse momentum in pp collisions at  $\sqrt{s} = 13$  TeV with the ATLAS detector*, ATLAS-CONF-2016-052.
  - [2] ATLAS collaboration, *Search for squarks and gluinos in events with an isolated lepton, jets and missing transverse momentum at  $\sqrt{s} = 13$  TeV with the ATLAS detector*, ATLAS-CONF-2016-054.
  - [3] ATLAS collaboration, *Further searches for squarks and gluinos in final states with jets and missing transverse momentum at  $\sqrt{s} = 13$  TeV with the ATLAS detector*, ATLAS-CONF-2016-078.
  - [4] M. Dine, *Naturalness Under Stress*, *Ann. Rev. Nucl. Part. Sci.* **65** (2015) 43–62, [[1501.01035](#)].
  - [5] L. J. Hall, D. Pinner and J. T. Ruderman, *A Natural SUSY Higgs Near 126 GeV*, *JHEP* **04** (2012) 131, [[1112.2703](#)].
  - [6] ATLAS collaboration, G. Aad et al., *Observation of a new particle in the search for the standard model higgs boson with the atlas detector at the LHC*, *Phys.Lett.* **B716** (2012) 1–29, [[1207.7214](#)].
  - [7] CMS collaboration, S. Chatrchyan et al., *Observation of a new boson at a mass of 125 GeV with the CMS experiment at the LHC*, *Phys. Lett.* **B716** (2012) 30–61, [[1207.7235](#)].
  - [8] S. Cassel, D. M. Ghilencea, S. Kraml, A. Lessa and G. G. Ross, *Fine-tuning implications for complementary dark matter and LHC SUSY searches*, *JHEP* **05** (2011) 120, [[1101.4664](#)].
  - [9] H. Baer, V. Barger, D. Mickelson and M. Padeffke-Kirkland, *SUSY models under siege: LHC constraints and electroweak fine-tuning*, *Phys. Rev.* **D89** (2014) 115019, [[1404.2277](#)].
  - [10] J. Ellis and K. A. Olive, *Supersymmetric Dark Matter Candidates*, [1001.3651](#).
  - [11] J. L. Hewett and T. G. Rizzo, *Low-Energy Phenomenology of Superstring Inspired E(6) Models*, *Phys. Rept.* **183** (1989) 193.
  - [12] P. Langacker and J. Wang, *U(1)-prime symmetry breaking in supersymmetric E(6) models*, *Phys. Rev.* **D58** (1998) 115010, [[hep-ph/9804428](#)].
  - [13] C. T. Hill and E. H. Simmons, *Strong dynamics and electroweak symmetry breaking*, *Phys. Rept.* **381** (2003) 235–402, [[hep-ph/0203079](#)].
  - [14] N. Arkani-Hamed, A. G. Cohen, E. Katz and A. E. Nelson, *The Littlest Higgs*, *JHEP* **07** (2002) 034, [[hep-ph/0206021](#)].
  - [15] T. Han, H. E. Logan, B. McElrath and L.-T. Wang, *Phenomenology of the little Higgs model*, *Phys. Rev.* **D67** (2003) 095004, [[hep-ph/0301040](#)].
  - [16] I. Antoniadis, *A Possible new dimension at a few TeV*, *Phys. Lett.* **B246** (1990) 377–384.
  - [17] M. Cvetič, D. A. Demir, J. R. Espinosa, L. L. Everett and P. Langacker, *Electroweak breaking and the mu problem in supergravity models with an additional U(1)*, *Phys. Rev.* **D56** (1997) 2861, [[hep-ph/9703317](#)].
  - [18] D. A. Demir, G. L. Kane and T. T. Wang, *The Minimal U(1)' extension of the MSSM*, *Phys. Rev.* **D72** (2005) 015012, [[hep-ph/0503290](#)].
  - [19] U. Ellwanger, C. Hugonie and A. M. Teixeira, *The Next-to-Minimal Supersymmetric Standard Model*, *Phys. Rept.* **496** (2010) 1–77, [[0910.1785](#)].
  - [20] J. R. Ellis, K. Enqvist, D. V. Nanopoulos, K. A. Olive, M. Quiros and F. Zwirner, *Problems for (2,0) Compactifications*, *Phys. Lett.* **B176** (1986) 403–408.
  - [21] P. Langacker and M. Plumacher, *Flavor changing effects in theories with a heavy Z' boson with family nonuniversal couplings*, *Phys. Rev.* **D62** (2000) 013006, [[hep-ph/0001204](#)].
  - [22] WMAP collaboration, G. Hinshaw et al., *Nine-Year Wilkinson Microwave Anisotropy Probe (WMAP) Observations: Cosmological Parameter Results*, *Astrophys. J. Suppl.* **208** (2013) 19, [[1212.5226](#)].
  - [23] PLANCK collaboration, P. A. R. Ade et al., *Planck 2013 results. XVI. Cosmological parameters*, *Astron. Astrophys.* **571** (2014) A16, [[1303.5076](#)].
  - [24] E. Ma, *Particle Dichotomy and Left-Right Decomposition of E(6) Superstring Models*, *Phys. Rev.* **D36** (1987) 274.
  - [25] S. W. Ham, E. J. Yoo and S. K. Oh, *Explicit CP violation in a MSSM with an extra U(1)-prime*, *Phys. Rev.* **D76** (2007) 015004, [[hep-ph/0703041](#)].
  - [26] P. Langacker, *The Physics of Heavy Z' Gauge Bosons*, *Rev. Mod. Phys.* **81** (2009) 1199–1228, [[0801.1345](#)].
  - [27] G. Bélanger, J. Da Silva, U. Laa and A. Pukhov, *Probing U(1) extensions of the MSSM at the LHC Run I and in dark matter searches*, *JHEP* **09** (2015) 151, [[1505.06243](#)].
  - [28] G. Belanger, J. Da Silva and A. Pukhov, *The Right-handed sneutrino as thermal dark matter in U(1) extensions of the MSSM*, *JCAP* **1112** (2011) 014, [[1110.2414](#)].
  - [29] G. Corcella, *Phenomenology of supersymmetric Z' decays at the Large Hadron Collider*, *Eur. Phys. J.* **C75** (2015) 264, [[1412.6831](#)].
  - [30] G. Corcella and S. Gentile, *Heavy Neutral Gauge Bosons at the LHC in an Extended MSSM*, *Nucl. Phys.* **B866** (2013) 293–336, [[1205.5780](#)].
  - [31] P. S. Bhupal Dev, S. Mondal, B. Mukhopadhyaya and S. Roy, *Phenomenology of Light Sneutrino Dark Matter in cMSSM/mSUGRA with Inverse Seesaw*, *JHEP* **09** (2012) 110, [[1207.6542](#)].
  - [32] V. Barger, D. Marfatia and A. Peterson, *LHC and dark matter signals of Z' bosons*, *Phys. Rev.* **D87** (2013) 015026, [[1206.6649](#)].
  - [33] C.-W. Chiang, T. Nomura and K. Yagyu, *Phenomenology of E<sub>6</sub>-Inspired Leptophobic Z' Boson at the LHC*, *JHEP* **05**



- (2014) 106, [1402.5579].
- [34] G. Bélanger, J. Da Silva and H. M. Tran, *Dark matter in  $U(1)$  extensions of the MSSM with gauge kinetic mixing*, [1703.03275](#).
  - [35] J. Erler, *Chiral models of weak scale supersymmetry*, *Nucl. Phys.* **B586** (2000) 73–91, [[hep-ph/0006051](#)].
  - [36] F. Deppisch, A. Freitas, W. Porod and P. M. Zerwas, *Determining Heavy Mass Parameters in Supersymmetric  $SO(10)$  Models*, *Phys. Rev.* **D77** (2008) 075009, [[0712.0361](#)].
  - [37] J. E. Kim and H. P. Nilles, *The mu Problem and the Strong CP Problem*, *Phys. Lett.* **B138** (1984) 150.
  - [38] D. Suematsu and Y. Yamagishi, *Radiative symmetry breaking in a supersymmetric model with an extra  $U(1)$* , *Int. J. Mod. Phys.* **A10** (1995) 4521–4536, [[hep-ph/9411239](#)].
  - [39] M. Cvetič and P. Langacker, *New gauge bosons from string models*, *Mod. Phys. Lett.* **A11** (1996) 1247–1262, [[hep-ph/9602424](#)].
  - [40] V. Jain and R. Shrock,  *$U(1)$ -A models of fermion masses without a mu problem*, [[hep-ph/9507238](#)].
  - [41] D. A. Demir, *Two Higgs doublet models from TeV scale supersymmetric extra  $U(1)$  models*, *Phys. Rev.* **D59** (1999) 015002, [[hep-ph/9809358](#)].
  - [42] P. Minkowski,  *$\mu \rightarrow e\gamma$  at a Rate of One Out of  $10^9$  Muon Decays?*, *Phys. Lett.* **B67** (1977) 421–428.
  - [43] R. N. Mohapatra and G. Senjanovic, *Neutrino Mass and Spontaneous Parity Violation*, *Phys. Rev. Lett.* **44** (1980) 912.
  - [44] J. Schechter and J. W. F. Valle, *Neutrino Masses in  $SU(2) \times U(1)$  Theories*, *Phys. Rev.* **D22** (1980) 2227.
  - [45] J. Schechter and J. W. F. Valle, *Neutrino Decay and Spontaneous Violation of Lepton Number*, *Phys. Rev.* **D25** (1982) 774.
  - [46] J.-h. Kang, P. Langacker and T.-j. Li, *Neutrino masses in supersymmetric  $SU(3)(C) \times SU(2)(L) \times U(1)(Y) \times U(1)$ -prime models*, *Phys. Rev.* **D71** (2005) 015012, [[hep-ph/0411404](#)].
  - [47] D. A. Demir and Y. Farzan, *Correlating mu parameter and right-handed neutrino masses in  $N=1$  supergravity*, *JHEP* **03** (2006) 010, [[hep-ph/0601096](#)].
  - [48] D. A. Demir, L. L. Everett and P. Langacker, *Dirac Neutrino Masses from Generalized Supersymmetry Breaking*, *Phys. Rev. Lett.* **100** (2008) 091804, [[0712.1341](#)].
  - [49] S. Heinemeyer, O. Stal and G. Weiglein, *Interpreting the LHC Higgs Search Results in the MSSM*, *Phys. Lett.* **B710** (2012) 201–206, [[1112.3026](#)].
  - [50] G. G. Ross, K. Schmidt-Hoberg and F. Staub, *The Generalised NMSSM at One Loop: Fine Tuning and Phenomenology*, *JHEP* **08** (2012) 074, [[1205.1509](#)].
  - [51] F. Staub, *SARAH 4 : A tool for (not only SUSY) model builders*, *Comput. Phys. Commun.* **185** (2014) 1773–1790, [[1309.7223](#)].
  - [52] W. Porod and F. Staub, *SPheno 3.1: Extensions including flavour, CP-phases and models beyond the MSSM*, *Comput. Phys. Commun.* **183** (2012) 2458–2469, [[1104.1573](#)].
  - [53] G. Bélanger, F. Boudjema, A. Pukhov and A. Semenov, *micrOMEGAs4.1: two dark matter candidates*, *Comput. Phys. Commun.* **192** (2015) 322–329, [[1407.6129](#)].
  - [54] P. Bechtle, O. Brein, S. Heinemeyer, G. Weiglein and K. E. Williams, *HiggsBounds: Confronting Arbitrary Higgs Sectors with Exclusion Bounds from LEP and the Tevatron*, *Comput. Phys. Commun.* **181** (2010) 138–167, [[0811.4169](#)].
  - [55] P. Bechtle, S. Heinemeyer, O. Stål, T. Stefaniak and G. Weiglein, *HiggsSignals: Confronting arbitrary Higgs sectors with measurements at the Tevatron and the LHC*, *Eur. Phys. J.* **C74** (2014) 2711, [[1305.1933](#)].
  - [56] A. Buckley, *PySLHA: a Pythonic interface to SUSY Les Houches Accord data*, *Eur. Phys. J.* **C75** (2015) 467, [[1305.4194](#)].
  - [57] J. Erler, P. Langacker, S. Munir and E. Rojas, *Improved Constraints on Z-prime Bosons from Electroweak Precision Data*, *JHEP* **08** (2009) 017, [[0906.2435](#)].
  - [58] CMS collaboration, V. Khachatryan et al., *Search for new physics with the  $M_{T2}$  variable in all-jets final states produced in  $pp$  collisions at  $\sqrt{s} = 13$  TeV*, *JHEP* **10** (2016) 006, [[1603.04053](#)].
  - [59] PARTICLE DATA GROUP collaboration, C. Patrignani et al., *Review of Particle Physics*, *Chin. Phys.* **C40** (2016) 100001.
  - [60] ATLAS collaboration, M. Aaboud et al., *Search for top squarks in final states with one isolated lepton, jets, and missing transverse momentum in  $\sqrt{s} = 13$  TeV  $pp$  collisions with the ATLAS detector*, *Phys. Rev.* **D94** (2016) 052009, [[1606.03903](#)].
  - [61] LHCb collaboration, R. Aaij et al., *First Evidence for the Decay  $B_s^0 \rightarrow \mu^+ \mu^-$* , *Phys. Rev. Lett.* **110** (2013) 021801, [[1211.2674](#)].
  - [62] HEAVY FLAVOR AVERAGING GROUP collaboration, D. Asner et al., *Averages of  $b$ -hadron,  $c$ -hadron, and  $\tau$ -lepton properties*, [1010.1589](#).
  - [63] Y. Amhis et al., *Averages of  $b$ -hadron,  $c$ -hadron, and  $\tau$ -lepton properties as of summer 2016*, [1612.07233](#).
  - [64] G. Corcella, *Searching for supersymmetry in  $Z'$  decays*, *EPJ Web Conf.* **60** (2013) 18011, [[1307.1040](#)].
  - [65] R. V. Harlander, S. Liebler and H. Mantler, *SusHi: A program for the calculation of Higgs production in gluon fusion and bottom-quark annihilation in the Standard Model and the MSSM*, *Comput. Phys. Commun.* **184** (2013) 1605–1617, [[1212.3249](#)].
  - [66] LHC HIGGS CROSS SECTION WORKING GROUP collaboration, J. R. Andersen et al., *Handbook of LHC Higgs Cross Sections: 3. Higgs Properties*, [1307.1347](#).
  - [67] MUON G-2 collaboration, G. W. Bennett et al., *Final Report of the Muon E821 Anomalous Magnetic Moment Measurement at BNL*, *Phys. Rev.* **D73** (2006) 072003, [[hep-ex/0602035](#)].
  - [68] MUON G-2 collaboration, J. Grange et al., *Muon ( $g-2$ ) Technical Design Report*, [1501.06858](#).
  - [69] J-PARC G-2/EDM collaboration, N. Saito, *A novel precision measurement of muon  $g-2$  and EDM at J-PARC*, *AIP*

- Conf. Proc.* **1467** (2012) 45–56.
- [70] WMAP collaboration, E. Komatsu et al., *Seven-Year Wilkinson Microwave Anisotropy Probe (WMAP) Observations: Cosmological Interpretation*, *Astrophys. J. Suppl.* **192** (2011) 18, [[1001.4538](#)].
  - [71] WMAP collaboration, D. N. Spergel et al., *Wilkinson Microwave Anisotropy Probe (WMAP) three year results: implications for cosmology*, *Astrophys. J. Suppl.* **170** (2007) 377, [[astro-ph/0603449](#)].
  - [72] LUX collaboration, D. S. Akerib et al., *Improved Limits on Scattering of Weakly Interacting Massive Particles from Reanalysis of 2013 LUX Data*, *Phys. Rev. Lett.* **116** (2016) 161301, [[1512.03506](#)].
  - [73] M. Mitchell, B. Muftakhidinov, T. Winchen, Z. Jedrzejewski-Szmek and T. G. Badger, *engage-digitizer: Support for smaller monitors*, Aug., 2016. [10.5281/zenodo.61108](#).
  - [74] ICECUBE collaboration, R. Abbasi et al., *Limits on a muon flux from neutralino annihilations in the Sun with the IceCube 22-string detector*, *Phys. Rev. Lett.* **102** (2009) 201302, [[0902.2460](#)].
  - [75] H. Baer, V. Barger and A. Mustafayev, *Implications of a 125 GeV Higgs scalar for LHC SUSY and neutralino dark matter searches*, *Phys. Rev.* **D85** (2012) 075010, [[1112.3017](#)].
  - [76] C. Arina et al., *A comprehensive approach to dark matter studies: exploration of simplified top-philic models*, *JHEP* **11** (2016) 111, [[1605.09242](#)].
  - [77] C. Degrande, C. Duhr, B. Fuks, D. Grellscheid, O. Mattelaer and T. Reiter, *UFO - The Universal FeynRules Output*, *Comput. Phys. Commun.* **183** (2012) 1201–1214, [[1108.2040](#)].
  - [78] J. Alwall, R. Frederix, S. Frixione, V. Hirschi, F. Maltoni, O. Mattelaer et al., *The automated computation of tree-level and next-to-leading order differential cross sections, and their matching to parton shower simulations*, *JHEP* **07** (2014) 079, [[1405.0301](#)].
  - [79] T. Sjöstrand, S. Ask, J. R. Christiansen, R. Corke, N. Desai, P. Ilten et al., *An Introduction to PYTHIA 8.2*, *Comput. Phys. Commun.* **191** (2015) 159–177, [[1410.3012](#)].
  - [80] DELPHES 3 collaboration, J. de Favereau, C. Delaere, P. Demin, A. Giammanco, V. Lemaître, A. Mertens et al., *DELPHES 3, A modular framework for fast simulation of a generic collider experiment*, *JHEP* **02** (2014) 057, [[1307.6346](#)].
  - [81] M. Cacciari, G. P. Salam and G. Soyez, *The Anti- $k(t)$  jet clustering algorithm*, *JHEP* **04** (2008) 063, [[0802.1189](#)].
  - [82] M. Cacciari, G. P. Salam and G. Soyez, *FastJet User Manual*, *Eur. Phys. J.* **C72** (2012) 1896, [[1111.6097](#)].
  - [83] E. Conte, B. Fuks and G. Serret, *MadAnalysis 5, A User-Friendly Framework for Collider Phenomenology*, *Comput. Phys. Commun.* **184** (2013) 222–256, [[1206.1599](#)].
  - [84] M. Frank, L. Selbuz and I. Turan, *Neutralino and Chargino Production in  $U(1)'$  at the LHC*, *Eur. Phys. J.* **C73** (2013) 2656, [[1212.4428](#)].
  - [85] XENON collaboration, E. Aprile et al., *Physics reach of the XENON1T dark matter experiment*, *JCAP* **1604** (2016) 027, [[1512.07501](#)].